INVESTIGATION ON PHOTONIC CRYSTAL FIBER SENSING USING METALLIC RODS

A Thesis Submitted in Fulfillment of the Requirement for the Award of the Degree of

MASTER OF ENGINEERING

In

Electronics and Communication Engineering

Submitted By

Rupinder Kaur

801561024

Under guidance of

Dr.R.S.Kaler

Senior Professor and Deputy Director,

Thapar University

ELECTRONICS AND COMMUNICATION ENGINEERING DEPARTMENT

THAPAR UNIVERSITY, PATIALA, PUNJAB

JUNE, 2017

CERTIFICATE

I, Rupinder Kaur hereby declare that the work presented in this thesis entitled "**Investigation on Photonic Crystal Fiber Sensing Using Metallic Rods**" in fulfillment of the requirement for the award of degree of Master of Engineering submitted at Electronics and Communication Engineering Department, Thapar University, Patiala is an authentic record of work carried out under supervision of Dr.R.S. Kaler -Senior Professor & Deputy Director, Thapar University. The matter presented in this has not been submitted either in part or full to any other university or institute for the award of any other degree.

Rupinder Kaur

Date: 18/9/2017

(Rupinder Kaur)

Roll no. : 801561024

It is certified that the above statement made by the student is correct to the best of my knowledge and belief.

Date: 18/9/2017

Dr. R. S. Kaler

Senior Professor & Deputy Director

Thapar University

ACKNOWLEDGEMENT

To discover, analyse and to present something new is to venture on an untraded path towards and unexplored destination is an arduous adventure unless one gets a true torch bearer to show the way. I would have never succeeded in completing my task without the cooperation, encouragement and help provided to me by various people. Words are often too less to reveal one's deep regards. I take this opportunity to express my profound sense of gratitude and respect to all those who helped me through the duration of this thesis. I acknowledge with gratitude and humility my indebtedness to **Dr. R. S. Kaler, Senior Professor,** Electronics and Communication Engineering Department, Thapar University, Patiala, under whose guidance I had the privilege to complete this thesis. I wish to express my deep gratitude towards him for providing individual guidance and support throughout the dissertation work.

I convey my sincere thanks to **Head of the Department, Dr.Alpana Agarwal** as well as **PG Coordinator, Dr. Hem Dutt Joshi, Assistant Professor,** Electronics and Communication Engineering Department, entire faculty and staff of Electronics and Communication Engineering Department for their encouragement and cooperation. I shall be failing in my duties if I don't express my deep sense of gratitude towards **Mr.Balveer Painam,** Senior Research Fellow, Electronics and Communication Engineering Department, Thapar University for his inquisitiveness, insight and inspiration through the whole work.

My greatest thanks are to all who wished me success especially my parents. Above all I render my gratitude to the almighty who bestowed self-confidence, ability and strength in me to complete this work for not letting me down at the time of crisis and showing me the silver lining in the dark clouds. I do not find enough words with which I can express my feelings of thanks to my dear friends and seniors for their help, inspiration and moral support which went a long way in successful competition of the present study.

Rupinder Kaur

Roll No. 801561024

ABSTRACT

In the recent few years, the photonic crystals have offered a potential platform for a broad range of applications in many domains. Many photonic crystal fibers such as in nonlinear devices, fiber-optic communications, high-power transmission, fiber lasers, highly sensitive gas sensors, and other fields have recorded high values of throughput. There has been noteworthy contribution of such components in different fields of miniature sizes, compactness, long term stability etc. The photonic crystals consist of periodic dielectric structures that have alternative low and high values of refractive index components. There is repetition of refractive index values after particular time duration that is of the order of the wavelength of light. The objective of this dissertation is to design and analyse various light confining optical designs based on photonic crystal fibers. The transmission and propagation characteristics curves are studied with the help of electromagnetic beam envelopes and electromagnetic frequency domain for finding the shifts. For confining light in the core region, parametric sweep is added for finding the fundamental mode. This is done with the help of Comsol software. The transmission and propagation curves are for these structures are also investigated. The transmission of light can be studied with the help of Maxwell equations. The Maxwell's equations are solved using Finite Element Method (FEM) approach. These curves give information about the amount of light confined and traversed in the metallic rods.

Firstly, an optical elliptical resonator is presented having metallic rods in the core region. The elliptical resonator is optimized for its performance as generating three times more value of electric field norm than ring resonator. By introducing appropriate material having desirable refractive index, varying the geometrical parameters, the electric filed and transmission efficiency is increased which results in red shift of the resonance wavelength. These modifications help to achieve enhanced sensitivity and quality factor in the resonator. Among all the materials, Silicon Nitride seems to be the most appropriate choice based on the light transmission with an average sensitivity of 500 nm/RIU obtained by variation of refractive index and semi minor axis width.

Further, we investigated the design of seven layered hexagonal shaped photonic crystal fiber consisting of gold nanowires in the innermost layer. The PCF consists of particular values of

Lattice constants and refractive indices for attaining maximum confinement of light in the core region. Here three gold nano rods in each of the innermost layer air hole are employed for sensing applications. The graphs for different propagation constants are plotted as a function of resonance wavelength and results are analysed which reveals optimum effective area, zero dispersion wavelength plot, effective mode index values, minimum confinement losses and attenuation with respect to wavelength.

For the above designed structures, the EMBE AND EWFD methods are implemented using Comsol software, where these structures are analysed critically from the obtained results.

TABLE OF CONTENTS

LIST OF FIGURES

.

LIST OF TABLES

LIST OF ABBREVATIONS

1. One dimensional-**1D**
2. Two dimensional-**2D**
3. Three dimensional -**3D**
4. Photonic crystal-**PC**
5. Transverse Electric- **TE**
6. Transverse Magnetic-**TM**
7. Photonic Band Gap- **PBG**
8. Silicon-on-Insulator-**SOI**
9. Photonic Crystal Fibres-**PCF**
10. Total Internal Reflection- **TIR**
11. Fiber Optic Systems - **FOS**
12. Refractive Index –**RI**
13. Signal to Noise Ratio - **SNR**
14. Refractive Index Unit-**RIU**
15. Finite Difference Time Domain-**FDTD**
16. Silicon dioxide-**SiO2**
17. Silicon Nitride- **Si_3N_4**
18. Electromagnetic Waves Frequency Domain- **EWFD**
19. Figure of Merit - **FOM**
20. Effective Index Method- **EIM**
21. Liquid Core Ring Resonator- **LCORR**
22. Complementary Metal Oxide Semiconductor-**CMOS**
23. Finite Element Method - **FEM**
24. Zero Dispersion Wavelengths - **ZDW**
25. Effective Mode Index - **EMI**
26. Electron Volt-**eV**
27. Perfectly Matched Layer - **PML**
28. Infra-Red- **IR**
29. Silicon Carbide- **SiC**
30. Distributed Feedback - **DFB**
31. Primary Sampling Unit - **PSU**
32. Quality Factor-**QF**

33. Full Width Half Maximum-**FWHM**
34. Conductivity, Temperature, and Depth- **CTD**
35. Partial Differential Equation- **PDE**
36. Surface Plasmon Resonance- **SPR**
37. Electromagnetic Beam Envelopes- **EMBE**

CHAPTER 1
INTRODUCTION

A sensor is a device that detects or measures a physical quantity, and the types of sensors we are concerned with are the types of sensors whose output is electrical. The opposite device is an actuator, which converts a signal to some action, usually mechanical. A transducer is a device that converts energy from one form into another, and here we are concerned only with the transducers in which one form of energy is electrical. Actuators and sensors are therefore forms of transducers.

The differences between sensors and transducers are very minimal. A sensor performs action as a transducer, and the transducer must necessarily sense some physical quantity. The difference lies in the efficiency of energy conversion. The purpose of a sensor is to detect and measure, and whether its efficiency is 5% or 0.1% is almost immaterial, provided the figure is known. Linearity of response, defined by plotting the output against the input, is likely to be important factor for sensors, but efficiency of conversion is not much important.

1.1 WHY SENSORS?

Sensing is a key technology for application areas like entertainment, transport, health and other industrial uses. Such applications require the concept of remote sensors, where data is acquired from remote places. This concept requires three basic ingredients:-

- Sensor: - A device which provides information about the physical/chemical/biological quantity of interest (e.g., pressure, temperature, pH etc.) that can be easily transmitted and processed [1].
- Transmission Lines
- A platform to enable conversion of transmitted data into a format easily understood by human senses, i.e., displays that make the data visible or audible [1].

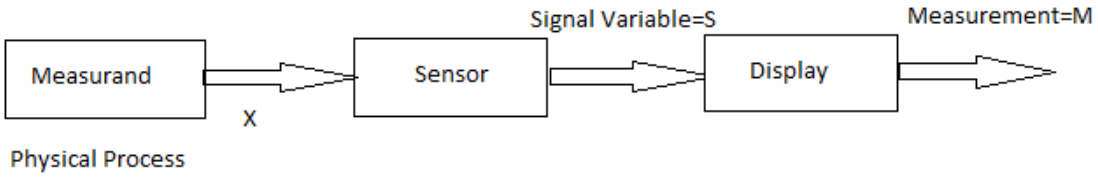

Figure 1.1 Simple instrument diagram of a sensor

The transmission lines generally employed are copper cables which are widely available so there is wide choice of selection among the various types of available sensors. The consideration of optical fibers as sensors, allow interaction of parameters that could be physical, chemical, or biological with light to generate a modulated optical signal containing information about the quantity to be measured. This format is easily accessed by the receiver with the help of a photo detector, which can convert light into the corresponding voltage or current**.**

1.1.1 Characteristics of Sensors

As sensors are incapable of replicating transfer functions which are ideal as there is chance of deviation which further reduce the accuracy [3].

- *Range* – It is defined as the highest and lowest value of operating range in which a sensor operates. Although sensors are capable of operating beyond this range but, for that extra calibration is required. For example- There are sensors employed to measure salinity in estuaries which have value in PPTs like 2PSU on PSU scale. But, if we use a sensor beyond its operating range like employ a pressure measuring sensor of 130m value at 200m depth then it alter the sensitivity or destroy the sensor.

- *Accuracy* – It is generally used to observe that how efficiently a sensor can measure the environmental variations means when comparison is made between the obtained data and recognized data. Example- If we have a temperature measuring sensor whose accuracy is 0.001^0C, then we expect the output to match or lie within 0.001^0C like that could be calculated by PRT standard or triple point of water cell and sometimes by a different sensor whose accuracy is almost similar. This is basically what is desired for comparison of results with the obtained observations.

- *Resolution* – There are different results obtained which have minimum variations in the outputs. For example in a sensor employed for temperature sensing, the resolution can be of 0.000,01º C but its accuracy is just 0.001º C. It reveals that minimum variations in temperature are much less than the sensor accuracy. Quantization is employed in digital signals to control resolution. This is function of sampling procedure and does not depend on sensor.

- *Repeatability* – The sensor has a capability of measuring the data again when it is placed back in the same atmosphere. Although it is having a direct relation with accuracy but, sometimes it is not much accurate although it can perform repeatability.

- *Drift* – In a sensor, there is variation in the lower values of frequency as the time changes. Drift is mostly linked with time period when the component was manufactured. The performance lowers as the device is aged. There are drift sensors which can be improved if they are operating smoothly, for example there are temperature sensors known as sea birds which float around 1 m^{o}C/yr and there is possibility of changing the float for obtaining more accuracy. It is observed that bio fouling is also responsible for drift cause which is not rectified that easily although attempts are made to enhance it.

- *Hysteresis* **–** It is generally seen that when a high and low linear input is provided to a sensor, the results achieved at output generally delay from the input data, for example out of two curves- one is achieved at high pressure whereas other one at low pressure. There are many pressure based sensors which are facing this difficulty but, generally side-lined by highlighting the positive aspects of it. Mostly, it is observed that in case of a CTD reading on deck is altered when deck is not used. It is concluded that this trouble is not because of the delay in the reaction time but due to the inbuilt characteristics of a sensor. Even in CTD, temperature sensing can be an issue.

- *Stability* – It is one more method of defining drift property. It means that there is defined output for every provided input. The factors like stability which can be long lasting or small period based are methods to define noise of sensor with variations in frequency. It is articulated as precision within certain duration. Although drift is an issue, if value of pressure is large in pressure sensors. As most of the sensors drift with duration of time therefore cells soften in gallium and triple point of water.

- *Response time* – It is time calculated during a straightforward approximation of response of frequency in a sensor by considering the behaviour to be exponential type.

1.1.2 Types of Sensors

According to the domain and type of magnitude to be calculated, sensors are categorised as:-

Mechanical: It includes extent of velocity, acceleration, displacement and pressure. There are seismic masses and membranes which produce optical effects which are employed for calculating volume.

Thermal: There is method of calculation of temperature dependence which is caused due to RI, emission spectra, transmission or effects of non-linear type like scattering that is produced in different components.

Electromagnetic: It is employed in photonic devices for calculating and transducing fields present in magnetic and electric type and it is used with help of electro optic and magneto optic impacts.

According to the spatial distribution of the measurand to be determined:-

Point: This is a type of sensor that identify at particular point as in case of measuring results at distinct positions.

Integrated: There is a sensor type in which integration of data from different components is done which finally gives one result.

Distributed: It is a type that permits calculation of data of specific component in regular fashion at all positions in environment. There is understanding of spatial mapping if sensor is capable of locating the spatial location and level with proper accuracy and precise value [4].

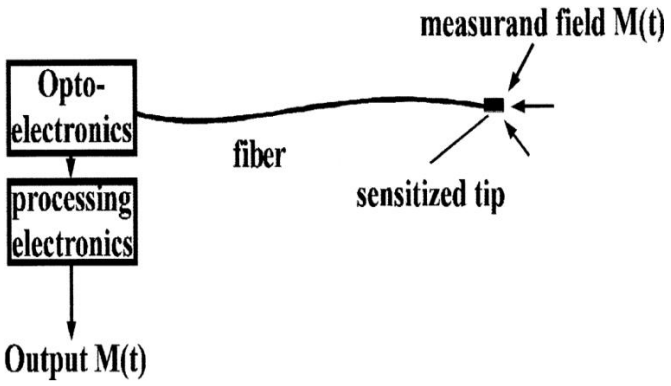

(a)

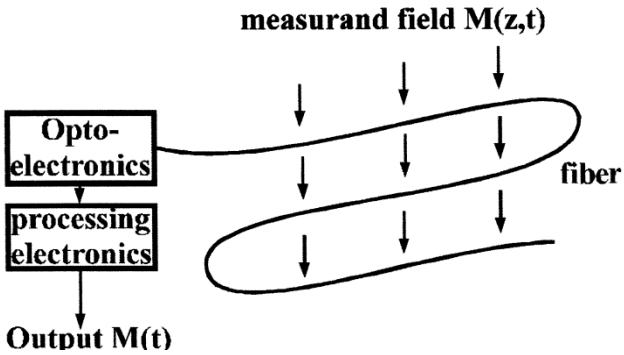

(b)

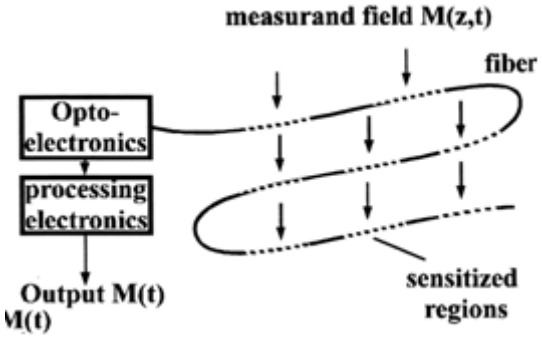

(c)

Figure 1.2 (a) Point, (b) Intrinsic, and (c) Distributed sensing

According to the nature of the transduction

Intrinsic: There are some categories of optical sensors where modification of intrinsic descriptive is performed which are further employed in waveguides of optical type as it is helpful in transducing techniques [6].

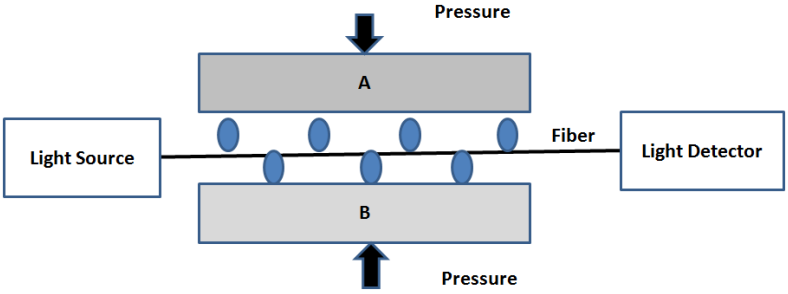

Figure 1.3 Intrinsic Sensors

Extrinsic: This type of sensors are employed for guiding light to a place which has sensation capability and where the signal enters in a different medium after moving from a cable. It is depicted that large variety of extrinsic sensors are present and in few situations we employ optical fiber for sending information to the acquisition from the sensor [7].

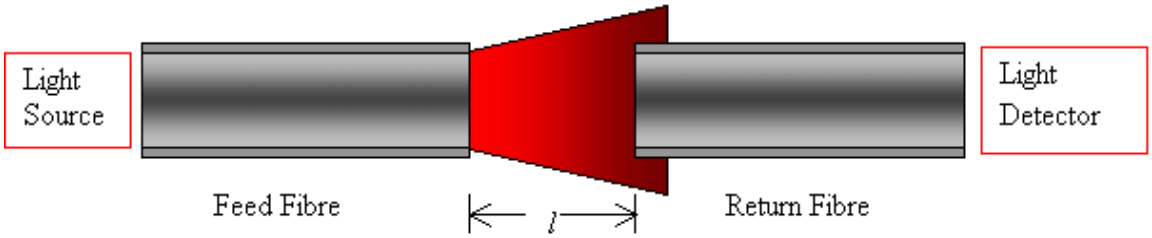

Figure 1.4 Extrinsic Sensors

According to the type of chemicals used

Bio Chemical Sensor: - It is a type of device employed for changing the chemical signal to an electrical state. Firstly, determination of chemical state is done with varying quantities, pressure, or with performance of components like atoms, molecular ions which are to be found in the solid, liquid or gaseous stage. It is analysed that chemical position of the atmosphere depicts the overall analytical configuration. There is classification of various biosensors on the basis of its characteristics which are employed for determining any specific component [8].

Biomedical Sensors: There exist varying categories of biomedical sensors like spectroscopic. We can compute the values of CO_2, oxygen and Ph at the same time. Further, laser dopplerimetry is employed for measuring the flow [6].

1.2 INTRODUCTION TO OPTICAL FIBERS

Optical fibers have transformed today's communication based industry and therefore it is chosen to be the first choice for telephones, security based cameras, net applications, and cable televisions. A huge transmitting capability of such optical fibers when joined with additional benefits, such as low losses, immunity to electromagnetic interference, small size, light weight, and electrical insulation, makes them the most efficient source of knowledge. Thus, there is wide spread use of such fibers not only in communication based industries but even in other fields [9].

Since last decade, there have been advancement because of progress in the field of optoelectronics and fiber based optic industries. For the progress of fiber optics, many studies have been performed by researchers that are basically related to particular designs. There was derivation of these results which resulted into recent innovations of sensing methods that employed optical fibers for further development of apparatus which used fibers as a base. As there is need of superior quality of fiber in the market so the prices of sensors have lowered and even the output has escalated as compared to previous years [1]. Therefore, on seeing such advancements in the conventional sensors there is replacement of magnetic and electric measurements, pressure, rotation, temperature, acceleration, vibration, strain, chemical calculations, angular position, viscosity, linear position, humidity and many other relevance have been motivated [10].

1.2.1 Anatomy of an Optical Fiber

An optical fiber consists of many layers as depicted in Figure 1.6. The innermost layer which is known as core is enclosed by cladding of fiber made of glass. In all cases, for proper transmission of light and to satisfy total internal reflection (TIR) condition, the value of refractive index of core is higher than that of cladding. The cladding is having different polymer layers for shielding the inner portions as there are chances of scratches, abrasion flaws due to moist conditions. These defects not only cause degradation of fiber but, even increase cracks. It is also depicted that in concrete substances whose pH value is high means basic in nature (pH = 12), there are chances of device getting corroded and reducing the life of fiber. Therefore, caution selection of polymer for protection is must [11].

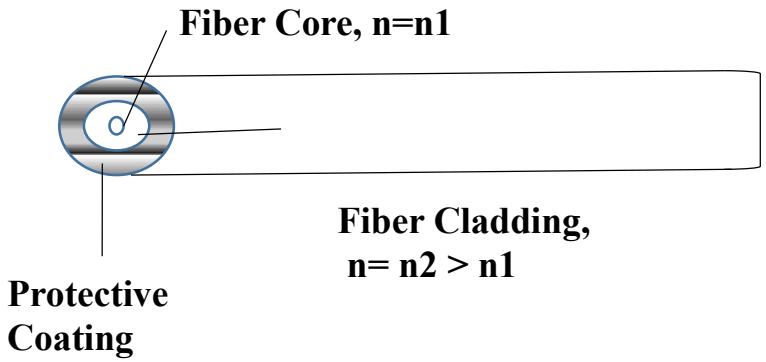

Figure 1.5 Schematic diagram of an optical fiber

Lastly, to reduce the bends in the fiber as it cause losses and even degrade fiber's performance, the polymer is chosen which has capability of absorbing stress. As it is observed that in telecom based industries, transmission losses occur due to micro bending so to avoid this proper selection of polymer is a mandatory step.

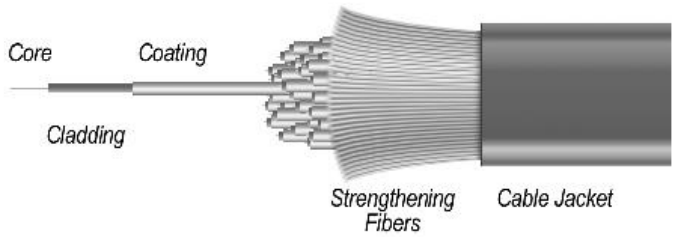

Figure 1.6 Different layers in Optical Fiber

The material employed for cladding is dielectric which has an index of refraction. It is mostly prepared with plastic or glass. There are different tasks performed by cladding like lessen the losses in the atmosphere from the core, it even prevent the outer part from absorbing the unwanted materials and also enhance the physical strength, minimize the scattering losses which take place at the core surface [13].

There is a coating known as buffer whose main function is just to shield the fiber from external harms like cracks, scratches. Mostly, plastic is employed for making the buffer. It is seen that buffer has elasticity which help in avoiding abrasion flaws [13].

The principle employed for guidance of light is TIR where a critical angle of incidence is present where TIR takes place. Whenever the incident angle is having higher value than the critical angle, there is complete reflection of light back in the glass source. For determining the value of critical angle of incidence a law is employed known as Snell's Law. In electromagnetic surface waveguides optical fiber is used [13].

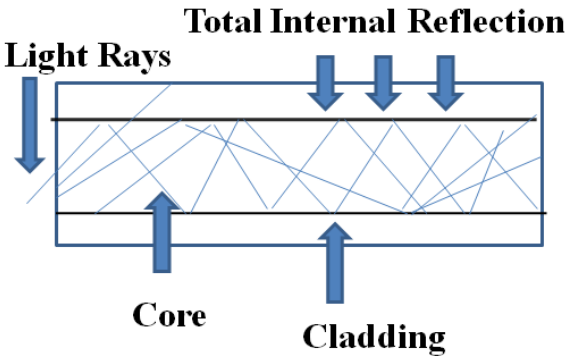

Figure 1.7 Total Internal Reflection

1.2.2 Advantages of Fiber Optics

- *Explosion Proof* - In this type of fiber there is no probability of electric shocks or sparks. Therefore, it is preferably employed in oil industries, medicinal usage as it can operate safely [14].

- *Immunity towards Radio Frequency and Electromagnetic interference:* As fibers are made of dielectric substances so there is no need of isolating them electrically and thus, they can be utilized in strong magnetic field, noisy environment by preventing electromagnetism and RF waves.

- *Environmental ruggedness and resistant:* As the material employed for making of fibers is glass or plastic so probability of getting corroded is least. Also, fibers can handle temperature's operating range from 350°C to 1200°C.

- *Small size, light weight and flexible*: The dimensions vary from 600 µm and can go up to 2.5µm in radius. Fiber has flexibility therefore there can be bending of up to 200µm when diameter is approximately 2cm. Therefore, it is employed in aircrafts.

- *Remote Sensing:* It is observed that when surroundings have unfavourable conditions, even there optical components can be transmitted till 1000m.

- *High Sensitivity*: It is analysed that there is availability of wide range of bandwidth and even value of sensitivity is high. We can obtain optimum results and many other additional benefits because of multiplexing characteristic of sensors.

- *Compactness:* There is accessibility of miniature sized sources and detectors which further prove to be beneficial for making of dense size sensors.

1.2.3 Modulation Schemes

There is broad classification of optical sensors according to the type of modulation used for signals.

- *Intensity Modulated Sensors*: - It is a type of modulator in which light from the source is transmitted which has light intensity function of the prevailing environment. The

condition required for efficient working of fibers is that there should be no cracks or bending during the transmission of signal as it is observed that the light intensity lowers and sometimes even weaken if there is a breakage at particular point. The structure of such type of modulator is easy and even price is low. For example crack sensor is example of intensity modulator [15].

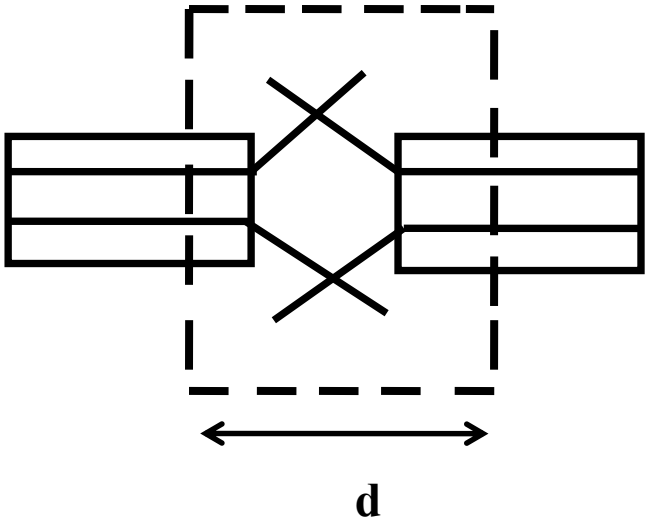

Figure 1.8 Intensity based optical fiber sensor

- *Phase Modulated Sensors*: - It is a type of sensor which employs idea of interference, where condition of phase matching is seen between reference and the sensing fiber. These sensors have perfect dynamic range and high accuracy as compared to intensity modulators, although has high prices. It also has some disadvantages as at the source, there is requirement for light to be coherent [15].

  The relationship between the optical path and the phase change is written as:-

$$\phi(r,t)=\frac{2\pi}{\lambda} L(r,t) \qquad (1)$$

  Where λ is the light wavelength and *L*(*r, t)* represents the optical path change.

- *Polarization Modulation based Sensors*: - This is an optical sensor where light is commenced to the fiber and further changes are deliberated that is required for final output that is as a parametrical function. It is observed that different parameters are present that has impact on light of polarization as because of magnetic field Faraday rotation occurs with an angle which is proportional to the field given at the source [15].

- *Fiber Optic Sensors based on the Mach–Zehnder Interferometer:* - It is a type of modulator consisting of reference and sensing arm. A coherent source is required for light like launching of (DFB) distributed feedback semiconductor into single mode fiber. The splitting of light having same intensity is done with help of directional coupler. One part of light is transmitted through reference arm and the other part is sent by the sensing arm. The output received when the light is transmitted through the reference and sensing arms, the results are joined at the directional coupler. Therefore, an interfering output among the two beams is created which is later employed for detection with the help of photo detector [16].

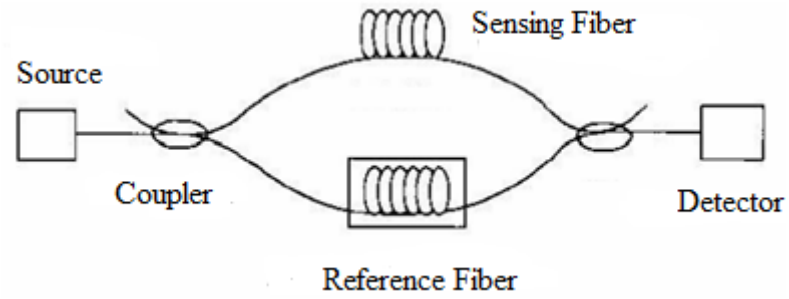

Figure 1.9 Mach Zehnder based optic fiber sensor

- *The Fabry–Perot Interferometer* as depicted in Figure 1.10 is a type of modulator which has multiple beams. The delay of phase is increased because of high reflection in the mirrors, light rebounds inward and outward in the empty space. The final result obtained at the Fabry Perot interferometer is defined according to the peak of interference whose value must be high as per the coefficient of reflection. It is depicted that results of light intensity are quite sensitive as per the variations in the phase changes, especially closer to peak area [16].

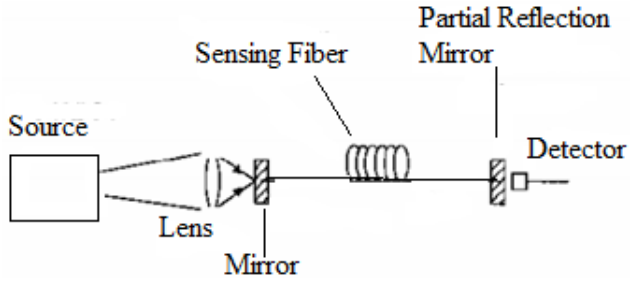

Figure 1.10 Fabry Perot based optic fiber sensor

1.2.4 Applications

There is a rapid advancement in the applications and further improvement in the technology of optical fiber sensors because of the positive results achieved in various fields [16].It is analysed that such recent innovations made by sensors has resulted in new measurement methods and even diversified strength in different areas. The areas which are highly affected with advancements in optical fiber sensors are electrical power based industries, chemical sensing areas, big concrete and composite arrangements and even the oil and gas refineries.

- *Applications to Large Composite and Concrete Structure:* - It is observed that FOS has many unique features as compared to conventional sensors as it can ability to withstand even in unfavourable conditions, the size of composites is very small therefore there are no disturbances in the features of the design, also there is prevention of corrosion in open space like dams and bridges. Such characteristics have enhanced controlling quality during health check-ups after building, building constructions, effect of huge concrete and composite designs. There are different areas like dams, bridges, aircraft and mines where such applications are employed [16].

- *Application in the Electric Power Industry*: - As it is known that Fiber Bragg Grating has resistance towards electromagnetic interference so it is readily employed in industries based on electrical concept. The measurement of power transformers for winding temperature, loading of power in transmission lines is done with this type of sensors [16].

- *Application in Medicine:* - It is observed that many sensors have electrical characteristics which mean they cannot be employed in medical areas because of electrical shocks. Therefore in such cases we employ FOS which have advantage over this because they have dielectric properties. For example, nowadays optical sensors are utilized for measuring efficiency of heart on the basis of method known as flow-directed thermo dilution catheter. This is known as Blood Monitoring. In eye related problems, for detecting cataract from the lens of eye, the backscattered light is monitored where autocorrelation method is employed for of alpha-crystallite aggregation.

- *Application in the Oil and Gas Industry*: - As FOS are safe due to its intrinsic nature, can operate at different temperature, have high immunity to electromagnetic interference,

ability to be multiplexed therefore, they are easily employed in gas and oil based industries for various applications [16].

So it is vivid that because of such widespread applications and advantages Optical sensors have gained interest as we have already mentioned it has miniature and dense structure, light in weight, easily multiplexed and most important is that there is no effect of electromagnetic interference. One of the most additional benefits is that there is no need of external power supply at the positions where sensing need to be done and lastly manufacturing is performed at less price [17].

1.2.5 Issues with Optical Fiber Sensors

As per the advantages of optical fiber sensors, it seems FOS is of immense value but, there are some drawbacks also as discussed:-

- *Cost*: The price is comparatively high as compared to electrical type of sensors.
- *Ambient Light*: As interference problem arises between the desired signal and the ambient light so to prevent it, the process must be performed in environment where light cannot reach.
- *Response Time:* The duration of obtaining results is increased when multiphase is employed.
- *Long-term Stability:* As we know this technology is recent so no wide knowledge of its output and long term processing is available.
- *Dynamic Range:* The range of electrical sensors is high as compared to FOS.
- *Data Interpretation:* It is noticed that it is difficult to handle the results obtained because there is variation in the results even when either of the parameter is altered. Thus, there is need to manage the alterations in the factors [1].

1.3 WHAT ARE PHOTONIC CRYSTALS?

There is evolution of new technology in the field of optics on the basis of optical fibers and waveguides. Photonic crystals are class of optics which is signified with artificial or natural designs which has modulation of refractive index in a periodic manner. This type of optics has some strange features like it provides chance of applications which can be employed on its basis [18]**.** PhCs have periodic designs for controlling the transmission of electromagnetic waves. It consists of two different components which have diverse dielectric constants as

shown in Figure 1.11. Among the two materials; the value of dielectric constant of one is ε_1 while the other has lower value of dielectric constant that is ε_2. There is one of the basic characteristic that photonic crystals comprise of that is electromagnetic waves which has frequencies in a certain period in which no waves are permitted to propagate in the given periodic design. This range where specific frequencies are not allowed to propagate is known as *Photonic Band Gap* [19].

1.3.1 Structural and Theoretical Model of Photonic Crystal

There has been a lot research in photonic optical structures and when we imply to structures other than 1-D it is known as Photonic crystals. On the basis of geometry utilized, photonic crystals are classified as one-dimensional (1-D), two-dimensional (2-D) or three-dimensional (3-D). Among these one dimensional are manufactured by depositing many layers, in two dimensional type holes are drilled in suitable materials and in three dimensional, holes are drilled at certain angles [20].

In 1-D Photonic crystals, there is periodicity of modulation of the permittivity which takes place in particular path, whereas in remaining directions the design is uniform. In present times, these types of designs are employed for lowering reflectance from the plane means as antireflection and further help to enhance the quality of prisms, lenses and even many other optical devices [21]**.** But, it is depicted that most of the examinations linked to control of the radiating field are decided on the basis of 2-D and 3- D PhCs because they prove to be helpful in providing physics for fields which radiate light.

In two dimensional photonic crystals there is large number of different designs as they have periodicity of the permittivity in 2 different directions whereas in the remaining side there is uniformity in medium [19]**.** One of the most common examples of 2-D photonic crystals is silicon having porous design with holes arranged in periodic fashion that is represented by etched holes in silicon substrate. 2-D PhCs are excessively employed as cladding for non-linear appliances in the optical fiber [20].

The three dimensional photonic crystals have permittivity modulation in all the three given directions. The number of possible designs is comparatively large in 3-D as compared to one and two dimensional photonic crystals. There have been many researches for invention of latest

designs in 3-D which further enhance their applications in different areas. By altering the geometry of 3-D structures, different designs of lattices can be made. It is seen that three dimensional structures are almost same as solid state crystals; therefore they have same names and lattices [19].

Figure 1.11 Design of 1-D, 2-D and 3-D photonic crystals

1.3.2 Properties of Photonic Crystal Fibers

There are large number of alterations in air holes designs and their arranging patterns which provide ability of controlling the RI difference between the cladding and core of the optical fiber. This enhances characteristics of photonic crystals and even provides properties which were not present in traditional fibers. Therefore, it is employed in many applications. It is depicted that there are distinctive features in hollow and solid cores of fibers [20].

- *Dispersion:-*The broadening or extension of frequency or wavelength is known as dispersion. It is observed that because of certain drawbacks of traditional fibers similar properties are not achieved in photonic crystal fibers because of elasticity in the air holes which are located at particular positions, we can modify dispersion. If we increase the size of air holes, then there can be shifting of wavelength dispersion from zero to visible range.

- *Non- Linearity:* - If we confine the intensity in the core then the non-linear property of optical fiber is improved. It is observed that photonic crystal fibers act as a good medium for super-continuum generation during transmission from a non- linear medium.

- *High Birefringence*: - There is no effect of temperature on birefringence in photonic crystal fibers. It is observed that with minor variations in geometry of air holes, there can be large range of birefringence. We achieve birefringence because of refractive index which is distributed non-asymmetrically which is further dependent on spatial distribution and size of the air holes.

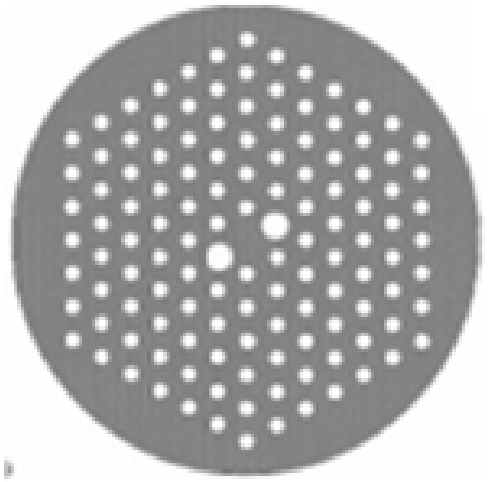

Figure 1.12 Birefringent PCF with hexagonal lattice

- *Large Mode Area***:** At specific wavelength, the value of Mode Field Diameter (MFD) can be same for PCF and Traditional fiber core. It is depicted that for wide range of frequencies the photonic crystal fiber is single mode whereas traditional fiber begin to behave as multimode near the allotted wavelength. If we want to achieve large mode field diameter then holes in the core need to be replaced with rods in photonic crystal fibers.

- *Hollow-Core Fiber*: The value of refractive index in the core which contains air is less as compared to refractive index of cladding. The propagation of light in such type of fibers takes place with help of mechanism known as Photonic Band gap. As it is vivid that transmission of small quantity of light is possible from the glass therefore the factors and their impacts like dispersion, scattering etc. which are concerned with light and glass are decreased up to greater extent.

1.3.3 Applications

As with minor variations and because of distinctive features of PCF, photonic crystal fibers are gaining popularity in diverse areas like in technical and scientific fields [20].

- As PCFs have the feature of positive dispersion so it can be employed for compensating the undesirable values of dispersion in telecommunication field.

- Nowadays, photonic crystal fibers can be utilized for devices which have non-linearity as a feature and support dispersion up to desired extent and this application is gaining wide popularity in present times.

- The insensitive nature towards temperature when we obtain birefringence is an essential element and therefore it is preferred in all applications.

- When there is requirement of transmission of any particular valued wavelength or wide band of spectrum of light then hollow core is preferred as it has wide applications in biology, medicine and many other areas.

1.4 MAXWELL EQUATIONS

As photonic crystals are defined with dielectric permittivity that is ε_r (x, y, and z) which is considered real and has periodicity in N direction and further does not change in the 3-N directions which are perpendicular to each other. The physical process related with travelling of electromagnetic waves in various components is illustrated mathematically by different set of differential equations called Maxwell's Equations [20].

In almost all cases, the materials employed for wave propagation have electrical current passing from them or can also be charged. But, there are some cases in which waves travel in materials where no free electrical charge or current is present. The Maxwell equations can be written in integral and differential form both. The differential form is described below [18]**.**

DIFFERENTIAL FORM

$$\nabla . \mathrm{D} = \rho, \quad \text{(Gauss's law)} \quad (2)$$

$$\nabla \times \mathrm{E} + \frac{\partial \mathrm{B}}{\partial \mathrm{t}} = 0, \quad \text{(Faraday's law of induction)} \quad (3)$$

$$\nabla . \mathrm{B} = 0, \quad \text{(Gauss's law for magnetism)} \quad (4)$$

$$\nabla \times \mathrm{H} - \frac{\partial \mathrm{D}}{\partial \mathrm{t}} = \mathrm{J}, \quad \text{(Ampere's circuital law)} \quad (5)$$

Where **E** and **H** are the electric and magnetic field vectors respectively, **D** and **B** are the electric displacement and magnetic induction field vectors, ∇ represents the gradient operator and $\partial/\partial t$ is the partial derivative with respect to time. D and B can be written in the form of relative permeability μ_r and dielectric constant ε_r as:

$$\mathrm{D} = \varepsilon_o \varepsilon_r \mathrm{E} = \varepsilon \mathrm{E} \quad (6)$$

$$\mathrm{B} = \mu_0 \mu_r \mathrm{H} = \mu \mathrm{H} \quad (7)$$

In a free space, μ_r and ε_r depend on the frequency. But if we consider that the system is free of sources and there is no dispersion, the Maxwell's equations change.

1.5 METHODOLOGY

The various arrangements of PhCs employed for applications related to sensing are structured with help of software- COMSOL. A concise introduction related to this software is detailed below.

COMSOL MULTIPHYSICS is defined as a type of software employed for finite element analysis, simulations and solving different engineering and physics based applications. It is also employed in coupling systems related to PDEs. Here we can enter the values of partial differential equations straight forward. The basic components of this software are the Application builder and the Model Builder. In the model builder, all the components to be employed and model are described like solving steps, examination of outputs and creation of

reports. We use application builder for creating applications which have specific user interface which can be easily used. The application is linked with the model we have created along with the model builder.

1.6 OBJECTIVE OF DISSERTATION

The most important objectives that have been analysed in this dissertation for designing hexagonal shape based on photonic crystal fiber and optical resonator are discussed below:-
To enhance sensitivity using metallic rods in an optical elliptical resonator and further improve transmission spectrum and quality factor.
For high sensing performance using selectively filled solid core photonic crystal fiber with gold nanowires and evaluating the propagation characteristics within certain described range of wavelength.

1.7 ORGANIZATION OF DISSERTATION

The thesis has been divided into the following chapters. The objective of each chapter is defined concisely as follow:

Chapter 1 as we have already elaborated all the basics needed to understand the characteristics of light travelling in a photonic crystal fiber and to solve the Maxwell's equations to numerically investigate the problem. Remaining work is structured as follows.

Chapter 2 discusses the literature survey done for the understanding of conceptual of photonic crystals as well as to describe the main objectives of the thesis. The researches of different authors are analysed comprehensively to know different techniques and practices for obtaining the various desired results. And therefore, we find gaps in their works and aim at enhancing the designs further.

Chapter 3 of the thesis focuses on an elliptical resonator having metallic rod in the core region instead of ring shaped for obtaining nearly three times greater value of electric field norm and further by varying the minor axis of the design transmission efficiency is increased rapidly. This chapter also explains that higher efficiency helps to obtain greater value of sensitivity and

further, wavelength resonances are shifting towards higher wavelengths that are red shift is obtained. The embe simulations are carried out using Comsol Multiphsyics software. This chapter fulfils both first and second objective.

Chapter 4 investigates the design of a seven layered hexagonal shaped photonic crystal fiber which consists of gold nanowires in the innermost holes. It is examined that by changing the structural parameters of the design, propagation characteristics such as, confinement loss, dispersion, effective mode index, attenuation and effective area, having desirable values can be obtained by varying the lattice constant in the desired range of wavelength with help of finite element based technique.

Chapter 5 finally, the entire work is concluded and further, recommendations for future scope by employing proposed designs are provided.

CHAPTER -2

LITERATURE REVIEW

Nowadays, Photonic Crystal Fiber, also known as microstructure fiber which has combined properties of both optical fiber and photonic crystal has gained much interest because PCFs have found application in numerous fields like fiber optic communications, fiber lasers, nonlinear devices, high-power transmission, sensors, and other areas. Due to its ability to confine light in hollow core as well as solid core fiber in different ways and altering characteristics by structural modifications it is far better than conventional fibers.

Xiang Yong Fu *et al*. [22] here to obtain surface Plasmon resonance sensors and overcome the complications and difficulty of coating the holes in the photonic crystal fiber, silver nanowire filled photonic crystal fibers are designed. Further, in areas of resonant wavelength and intensity detection sensing properties are discussed along with calculation of optical field distributions at various wavelengths using Finite Element Method. It is revealed that proposed designs give excellent effect having higher range of spectral and intensity sensitivity. Also, there is no requirement of coating process during the fabrication process.

Ying Lu *et al.* [23**]** proposed that photonic crystal fiber (PCF) having with different numbers of silver nanowires is used for sensing properties and surface Plasmon resonance by employing the finite element method (FEM) by using the COMSOL Multiphysics software. It is revealed that intensity sensitivity is directly dependent on the number of nanowires and distance between the nanowires. Further, calculations reveal that sensitivity is enhanced by 70 RIU_{-1} when the distance between the nanowires increased. Even the sensitivity is escalated if the number of nanowires is more than one because there is more interaction of electromagnetic field between the silver nanowires. Also, it is beneficial for practical considerations that there is no effect on sensitivity of the irregularities of filled nanowires.

Yang Peng *et al*. [24] demonstrated a SPR-based temperature sensor supported by photonic crystal fibers (PCFs). For enhancing the sensitivity, a liquid having high value of thermo-optic coefficient was employed in the second layer which consisted of air holes and even few of the

air holes are metal coated. Further values of the losses had been calculated by varying temperature that induced variations in the efficiencies of coupling among the different modes. There is proper consideration of the changes made in the values of dielectric constants of metal used, liquid filled in the air holes and fused silica. It is proposed that such temperature based sensor will be beneficial in chemical and medical fields as value of sensitivity is obtained as high as 720 pm⁄°C. The design did not consist of any packaging and phase matching problems.

Yang Peng *et al.* [25] proposed a simple and compact sized all-fiber temperature sensor based on selectively liquid-filled photonic crystal fiber (PCF) with utilization of proper under-controlled whole collapsing during post –processing of PCF. In the design, all the holes are filled with air except the innermost ring which had higher value of refractive index of the liquid filled in it. Further, in the sensor a Band gap like effect which has higher value of refractive index is analysed. With the usage of BG-effect, experimental results having high sensitivity nearly −5.5 nm⁄°C is achieved by filling the PCF with colloids of gold and dimethyl sulfoxide. It revealed that loss spectra of absorption were very sensitive to the liquids' refractive index which was lossless.

Y. Lu *et al*. [26] demonstrated a temperature sensor on the basis of photonic crystal fiber (PCF) which has certain positive aspects as its LMA-8 PCF was filled with nano sized wires and further, varying concentration of analyte is added for theoretical and experimental results. A blue shift was obtained as the temperature increased and even value of confinement loss and resonance wavelength varied at varying concentrations. A high value of temperature sensitivity was achieved when experimental simulations were studied and that could be used as a platform for future applications in temperature based or other type of sensors.

Nannan Luan *et al*. [27] designed a SPR based temperature sensor by employing silver nano sized wires as the filling material in the six- holes photonic crystal fiber (PCF). For providing a sensing medium, a colloidal consisting of ethanol and chloroform is filled into the holes as it has high value of thermo-optic coefficient. A shift in the resonance peaks is obtained when variations in the refractive indices are induced due to temperature changes. With the measurement of peak variations, temperature changes can be observed. As the refractive index

of filled liquid is very close to the refractive index of the material used in PCF so the peak at resonance is very sensitive. Further, the sensitive range is tuned by varying the ratios of the filled liquid mixture and it is made stable by filling random nano sized wires which further makes the fabrication of sensor easy.

Wei Du and Feng Zhao [28] proposed a design for an optical sensor waveguide which employed a semiconductor which has wide band gap that is silicon carbide (SiC). The benefit of choosing a material having large value of energy band gap is that it helps the waveguide to function in the near infrared and visible region. By employing the effective index method (EIM), the evaluation of sensing properties is done with help of confinement factor present in the transverse magnetic mode (TM_0). It was depicted that an improved value of confinement = 0.95 can be obtained which is not possible in non-SPR structure which is nearly 3.3 times more. This enhanced sensing is not only beneficial for bio-sensing and chemical sensing but, even compatible for SiC and Si based devices.

Qiang Liu *et al*. [29] presented a temperature sensor having a coupling in SPP and core mode with a high-sensitivity photonic crystal fiber (PCF) and simulations were carried by employing finite element method (FEM). In the innermost hole of the photonic crystal fiber a material having temperature sensation is filled. The coating of all the air holes present in the structure is done with nano-sized gold film. For making a core mode, six cores are required which are made with removal of air holes from the second layer. When phase matching condition between core and SPP mode is fulfilled, coupling takes place. A high value of linearity (0.99991) and sensitivity (-2.15nm/°C) is achieved when fiber length is taken to be 1mm. This temperature based sensor is in competition with other sensors in this field.

Clemens J. Kruckel [30] proposed a nitride enriched platform for optical components which are non-linear and have high integrity. To manufacture low stress silicon platform CMOS is utilized and further, high content of silicon helps to reduce tensile stress and provides easy growth of crack rid layer. Also, a high value of nonlinear Kerr coefficient is obtained that is nearly 5 times as compared to stoichiometric type. A tighter confinement is achieved with minimum bending of radii with refractive index = 2.1 and wavelength = 1.55μm. Further,

thorough evaluations depict accurate dispersion low scattering losses. Lastly, a high quality factor is achieved by micro fabricating the resonators.

Su Judith *et al.* [31] detected nano - sized particles as detection of a single molecule is the greatest confront in today's biology. These experiments mostly employ labels which are of high price, production is tedious, and it can disturb the events in molecules for undersized analyses. For determination of delectability, size of analyte is crucial factor. The improvement of signal to noise ratio (SNR) is important which is done with laser frequency locking by detecting nano sized particles in desired solutions. The analyses include various sizes of particles that vary from 2nm – 100nm which is beneficial for binding of particle during the frequency shift. This shift contributes to escalation of length of path that helps in coupling. Further, it anticipated that the analyses will provide more accurate diagnostics and studies in future.

Qiang Liu *et al*. [32] demonstrated a filter having index solutions in the inner hole of photonic crystal fiber (PCF) of a tunable polarized fiber. Finite element method (FEM) is used for simulation and evaluation of characteristics of loss spectra and dispersion of polarised filter. The filling of gold wires in the air holes of cladding is performed selectively. For coupling of surface Plasmon polarization (SPP) and liquid core mode, matching of phase condition is necessary. When there is variation in the parameters of structure and liquid, the resonant wavelength also alters. The realization of polarised filter occurs at varying wavelengths with adjustments in refractive index. It is condemned that for the first time that a narrowband filter operating at 1.31μm is designed that has FWHM = 16nm. The value of birefringence is comparatively good than earlier designs which are beneficial for separating positions of resonance wavelength at different modes. Lastly, it is depicted that resonance losses decrease with increase in distance in core and gold wires placed.

Felix Eltes *et al.* [33] presented a waveguide having low loss for non-linear photonics where waveguide is made of barium titanate ($BaTiO_3$) as it is famous material for extending functions of silicon in photonics. Here integration of $BaTiO_3$ on silicon on insulator (SOI) is designed with help of slot waveguide based geometries for both electro-optic and passive photonic

structures. As already existing devices are suffering from different type of propagation losses that further constraints its performance but, in this reasons of such losses are studied and alternatives are suggested by fabricating $BaTiO_3$ – Si based waveguide. For depositing epitaxial $BaTiO_3$, strontium titanate (SrTiO3) is employed. The manufacture of slot waveguide designs is done by providing exposure to hydrogen as it helps in absorption. Thus, extremely high speed non-volatile silicon based optical devices and switches can be designed.

Jeremy D.Witmer *et al.* [34] presented a design which is prepared with a material consisting of combination of Silicon/Lithium Niobate for a resonator of photonic crystal type. It is proposed that with help of index contrast in silicon and lithium niobate, there can be confinement of resonances in photonics made of slight film on lithium niobate. An electro optic coupling of 0.6 GHz/V is achieved with electrodes patterned with specific dimensions.

Chao Liu et al. [35] demonstrated a structure on the basis of surface Plasmon resonance (SPR) with help of a sensing metal that is gold. This design is comparatively simple because here gold is deposited on outer layer of fiber rather than filling in the core. The simulations are carried out by using finite element method. The sensing properties of PCF-SPR are affected by variations in the thickness of deposited gold, RI of analyte being added and dimensions of inner hole. Later, to achieve highest spectral sensitivity a grapheme is coated on gold film.

Md. Faizul Huq *et al.* [36] designed a structure for high sensitivity which comprised of a hexagonal shape photonic crystal fiber (PCF), further the structure size chosen is micro. The results are computed by using finite element method (FEM) having full vectorial length. In the prescribed design, computations are done in four levels. The technique opted for high sensitivity is by extending the radius dimensions of the holes present in the cladding. The sensitivity is further enhanced by employing one channel because accumulation of more channels degrades the sensitivity. Lastly, even the losses related to confinement can be reduced by employing varying dimensions.

X. C. Yang *et al*. [37] represented a sensor on the basis of both theoretical and experimental analysis by employing PCF containing silver nano - sized wires and liquid. A blue shift is observed by raising the temperature and further, by compromising the ratio of liquids added, resonance intensity and wavelength is tuned easily. For determining the performance of sensor, a wide range of temperature (25 °C to 60 °C) is predicted with varying ratios. Even high sensitivity and figure of merit (FOM) is achieved. It is possible to sense the remote positions with help of all-fiber device as it is mechanically stable. So, by varying length of down lead fiber, optimum results for real-time with high sensitivity can be obtained for temperature sensing.

Jitendra Narayan Dash *et al*. [38] demonstrated a biosensor which constituted of polymethyl methacrylate on the basis of photonic crystal fiber (PCF) which employed SPR. Here to match the condition of phase between core guided and Plasmon mode, the designed sensor comprises of an inner hole and air holes at cladding. An analyte is present in the indium tin oxide (ITO) which is coated at the air holes of second layer. It is reported that for high efficiency a minimum of 70nm thickness of ITO is required. This design revealed high resolution nearly $5 \times 10{-}5$ RIU along with sensitivity around 2000nm/RIU.

Min Huang *et al.* [39] introduced a latest scheme for sensor which consisted of nano-fluidics and nano- photonics by using free-standing crystals on one platform. It is analysed that manipulation of light and fluidics is possible both on theoretical and experimental basis by simply connecting openings of nano-size. A pivotal method for detecting refractive indices in aqueous solutions is present. It is revealed that rapid delivery of flow enhances sensitivity reaching up to 510nm/RIU when resonant wavelength is 850nm in solution. Further, if cross polarization techniques are used and SNR is increased then limit of detection can be enhanced.

X.C. Yang *et al.* [40] presented a glucose sensor consisting of nanowires made of silver in a photonic crystal fiber. The designed sensor is studied by experiments and evaluated with help of software - COMSOL multiphysics. It is depicted that sensitivity of spectrum (19009.17nm/RIU) in that is approximately equal to amount of glucose in water. The size of sliver nanowires employed in the design is taken under consideration as it has wide impact on

sensitivity. Therefore, size is fixed between 90-120nm. It is expected that optimum results for sensing glucose and efficient measurements can be done.

Shweta Saboo *et al.* [41] discussed a recent type of optical fiber that is photonic crystal fiber (PCF) on the basis of photonic crystals. It is beneficial due to certain characteristics like light confining ability and therefore being utilized in nonlinear devices, fiber lasers etc. Here loss related to confinement is calculated which is based on pitch, diameter, shape and pitch of holes. It is mandatory to eliminate this loss for confining the information in the centre because otherwise information gets dispersed. Thus, a PCF consisting of four layers is designed which has varying radius values.

Hongying Zhu *et al.* [42] demonstrated and analysed the detecting ability of the core optical ring resonator for biochemical sensing applications. Firstly a linear and basic connection between the response of liquid core ring resonator and its refractive index is developed. That further helps to detect the sensing capability of the LCORR. The testing of bio sensing is one with LCORR and bovine serum albumin (BSA) which have varying refractive index. There is a valid relation between theoretical and experimental results carried out. Further, obtained data reveals that Liquid core optical ring resonator can detect bovine serum albumin that has pictogram/mm^2 detecting limit.

Feng Hao *et al.* [43] presented that there is concentric arrangement between the ring and disk in the plasmonic nanocavities that has associated field enhancements and greater value of sensitivity of refractive index. In designs which have unequal symmetry, along with there is tunability feature named as Fano interference that is classified by using analytical harmonic oscillator. Further, there is investigation of spectral based resonances in the band of mid infra-red and visible spectrum which is beneficial for wide area applications based on surface spectroscopes.

Yuze Sun *et al*. [44] discussed the recent advancements made in optical based ring resonators that are employed as latest sensing technique for detecting analytes in gaseous and liquid contents. In this paper, the basic method used and analysing the different designing methods,

views of the present research on going and depicts the applications where ring resonators can be employed.

Lishuang Feng *et al.* [45] demonstrated a ring resonator which had silica waveguide along with transmissive optic gyro whose stability is enhanced. The descriptive study of transmissive resonator employed in TROG is done in this paper. There is an analysis of polarization which depends on resonator and further affects the residual modulating intensity of phase modulator. There is proper simulation, designing, fabrication, testing and developed the methods for building of transmissive resonator optic gyro. In this it is revealed that stability of nearly 0.22% within duration of 10seconds is achieved. Also, not much drift is obtained therefore it has large duration drifting characteristics.

Alireza Dolatabady *et al*. [46] demonstrated the characteristics of a nano - sized sensor based on its refractive index having 2-D plasmonic wave structure which consisted of small disk resonator and further employed Finite difference time domain (FDTD) for simulations. Later on, the analyses reveal a linear relationship between the RI of material which is to be sensed and resonating wavelength of the small disk. The accuracy of sensor is dependent on the resonating wavelength on the system to be detected. It is analysed that this type of sensor can be utilized with help of efficient designing for identifying different materials like for bio sensors.

X Z Fan *et al*. [47] discussed one of the bio sensing application in which integration of micro sized disk resonator is done with a virus sort of particle named as TMV-VLP present at the receptor layer. The functioning of bio receptor layer is performed with particular peptides which encrypt distinctive recognizing affinities. There is issue of integrating bio receptors with sensing platform because they all have varying capability. The functionality of optical small sized disk for binding of antibodies with the receptor further, reveal shifting of resonating wavelength examining the label free sensing of the structure. Thus, this depicts the flexible nature of receptor and its use during integrated with different prevailing transducer platforms.

Gilberto A. Rodriguez *et al*. [48] presented an optical resonator on a waveguide made of leaky silicon for obtaining a good QF bio-sensor and small in size, further consisted of wide surface for improving the recognizing capability of chemical and biological particles. There is distinctive nature of resonator that is porous which permits particles to connect straight forward with the modes which are having proper guided nature. It is depicted that QF in thousands was achieved with diameter of 50μm for silicon based optical ring shaped resonator. When the resonator is exposed to solution having water and salt then sensitivity measured is 380 nm/RIU. Also, a precise detection limit was shown for nucleic acidic particles which had surface detecting sensitivity – 4 pm/nM.

Marco Liscidini *et al*. [49] discussed four waves mixing which was done spontaneously to produce photonic pairs in circular resonators as it was done earlier by other scholar. It is also depicted that the value obtained for generation rate was very high because of wrong description of a factor named as field enhancement.

Shaonan Zheng *et al*. [50] demonstrated a spectrometer embedded on the chip which has high resonating value and has tunability with micro sized circular resonator that is obtained by utilizing high QF and thermal optical effect of micro sized optical resonator. With these variations bandwidth of 19nm and resolution value = 0.15nm is obtained.

Nir Rotenber *et al.* [51] proposed a latest quantum technology employing optics by interfacing nano - photons in light and emitters. For examining the interacting nature of different emitters with the slotted waveguide circles, finite element method analysis was combined with quantum analytic. It is observed that emission improvement of 1300 and coupling output having value equal to unity was obtained for radius values = 1.44μm and QF = 27900. It is revealed that large and even small coupling can be achieved in emitter circular systems by varying the dimensions or adding losses in the ring for seeing the oscillating nature named as Rabi in the micro rings. Even, slotted circular waveguides can be employed for coupling emission in particular direction with efficiency nearly equal to one.

S.NO	NAME OF THE AUTHOR	TITLE OF THE PAPER	YEAR OF PUBLISH	CONTENT
1.	Ademgil. H., & Haxha, S.	Highly Birefringent Photonic Crystal Fibers With Ultralow Chromatic Dispersion and Low Confinement Losses	2008	Designed a PCF which had low confinement losses, chromatic dispersion and high birefringence. Even polarizing beat length data is examined in the PCF.
2.	Hameed Mohamed Farhat O. *et al.*	Modal Properties of an Index Guiding Nematic Liquid Crystal Based Photonic Crystal Fiber	2009	Discussed mode analysis computations for an index guided PCF and examined various parameters where high birefringence (0.012) along with flat dispersion was achieved.
3.	Faruk Md. Omar *et al.*	Effect of Lattice Constant and Air Hole Diameter on the Mode Profile in Triangular and Square Lattice Photonic Crystal Fiber at THz Regime	2010	Discussed a new method for guiding light by using air holes in the cladding of PCF. Further, the impact of changes in air holes radius and lattice constant is examined where improved confinement is achieved in THz range.

4.	Mc Elhenny *et al.*	Dependence of Frequency Shift of Depolarized Guided Acoustic Wave Brillouin Scattering in Photonic Crystal Fibers	2011	Presented the dependence of frequency in photonic crystal fibers through simulations. The range of PCFs is broadened where acoustic modes can be categorised.
5.	Revathi S. *et al.*	Analysis of Propagation Characteristics in Photonic Crystal Fiber Structure for large negative Dispersion	2012	Proposed PCF with semiconductor material in the core region in which variations in parameters help to achieve propagation features like effective index mode, effective area etc.
6.	Dudley *et al*	Solid Core Photonic Crystal Fiber For Super continuum Generation	2013	Designed a PCF having solid core in which results for dispersion characteristics and effective refractive index are represented
7.	Hossain Md. Sajjad *et al.*	Dispersion and Nonlinear Characteristics of a Photonic Crystal Fiber (PCF) with Defected Core and Various Doping Concentration	2014	Proposed Zero dispersion fiber which had Desirable dispersion characteristics with just 3.03μm^2 effective area which can be used for nonlinear applications.

8.	Nair AA *et al*.	Comparative Study of Octagonal Ring Photonic Crystal Fiber with GeO2 Doped Structure	2014	Proposed a solid core PCF with octagonal ring structured and achieved large mode area with the Highest value of refractive index of inner ring.
9.	Saghaei Hamed *et al.*	Mid infrared supercontinuum generation via As2Se3 chalcogenide photonic crystal fibers.	2015	Discussed results of rod filling and optofluidic methods where zero dispersion is achieved when inner most holes are made of As_2Se_3 based chalcogenide glass.
10.	Hong Kee Suk *et al.*	Analysis on Transition between Index- and Band gap-guided Modes in Photonic Crystal Fiber	2016	Presented optical characteristics of hybrid photonic crystal fiber and compared guided regions with reference band gap and index guiding PCFs.
11.	Siwicki Bartlomiej *et al.*	Nanostructured graded-index core chalcogenide fiber with all-normal dispersion–design and nonlinear simulations.	2017	Proposed an approach for designing graded index fiber consisting of chalcogenide. The effect of graded index and dimensions on dispersion features is analyzed.
12.	MA J. *et al.*	High-performance temperature sensing	2017	Designed a high performance sensor based on temperature by

		using a selectively filled solid-core photonic crystal fiber with a central air-bore		filling selectively. The output obtained has high sensitivity and mode coupling efficiency is varied.
13.	Flannery Jeremy *et al.*	Implementing Bragg mirrors in a hollow-core photonic-crystal fiber	2017	Proposed techniques for implementation of Bragg gratings in hollow PCF. A high reflectivity having value greater than 99.99% is obtained.
14.	Cassataro Marco et *al.*	Generation of broadband mid-IR and UV light in gas-filled single-ring hollow-core PCF	2017	Designed ultrafast super continuum in a single ring PCF which presents flat transmission and dispersion in IR and near regions which had energy in μJ.
15.	Chupao Lin *et al.*	Liquid modified photonic crystal fiber for simultaneous temperature and strain measurement	2017	Presented a liquid modified PCF for improved sensitivity = 14.72nm/°C by filling a liquid of higher refractive index in the three adjacent air holes in the core region.

Table 2.1 Review of work done in the past in field of PCF based applications

CHAPTER 3

SENSITIVITY ENHANCEMENT USING METALLICRODS IN AN OPTICAL ELLIPTICAL RESONATOR

3.1 INTRODUCTION

There has been rapid progress in the field of optical nano technology due to its nanoscale electronics and broadband photonics which has further motivated interest in metal and dielectric nano - sized structures such as bio-sensing, Bragg reflectors, metamaterials etc. because of their distinctive properties [67].

Among the photonic devices micro ring resonator has attracted tremendous attention in the last decade because of many advantages like for frequency selective devices it can act as a building block for integrating massive values that is beneficial for tuning of bandwidth filters, switches and laser components. The optical resonators is one of the most adaptable device for detecting the micro sized chemical and biological components in liquids that can be helpful in the field of drugs, environmental forecasting, medical treatments etc. by acting as a label free optical biosensor [68].

The ability of confining the light beyond a certain limit in optical resonators by fulfilling the dimension variations [69]. This offers the resonators the improvements to attain high transmission efficiency. In the past decades, in a ring resonator, the whispering gallery modes formed due to Total Internal Reflection (TIR) of the light along the curved boundary between the high and low refractive index (RI) media [70] and studied based on various ideas which enhanced transmission through resonators and nano - sized arrays [69]. Further, a simple plasmonic based refractive index sensor was designed by Alireza Dolatabady et.al whose coupling could be controlled but the variations in the refractive index were not possible [71]. Quality factor is also a big concern in this regard as more the variation of the quality factor can be achieved, it will provide a larger scope to integrate devices [72].

In this paper, we have proposed a design consisting of an elliptical resonator instead of a ring resonator and obtained nearly three times high value of Electric Field norm (V/m) and also obtained transmission spectrum having higher efficiency. These are achieved by varying refractive index value from 1.49 to 1.52 for two different dimensions of semi-minor axis and

Semi-major axis of ellipse. Further, the transmission and wavelength graphs are calculated using a 2D axis symmetric geometry through the Multiphysics COMSOL software. Also, sensitivity is calculated to examine the sensor's performance.

3.2 WORKING PRINCIPLE

As already discussed in Chapter 1, there is periodic variation of refractive indices of materials known as photonic crystals. With the variation in the refractive index of the analytes added, the sensitivity and quality factor changes, causing an alteration in the cut off wavelengths. Therefore, sensitivity can be calculated which is expressed as:-

$$S = \frac{\Delta\lambda}{\Delta n}$$

$\Delta\lambda$ is the change in cut-off wavelength,

Δn is the change in refractive index of the analyte

Equation shows that the change in wavelength is proportional to the dimensions of the minor axis that is the area that is available for sensing. Hence, sensitivity increases with the increase in dimension of the minor axis.

Further, Quality Factor can be calculated as follow:

$$Q = \frac{\lambda_p}{FWHM}$$

λ_p is the peak or dip value of wavelength

FWHM is the full width half maximum of the wavelength

3.3. SENSOR DESIGN

For optimization purposes, a general schematic of an optical elliptical resonator is shown in figure. It consists of two waveguides, the straight waveguide and an elliptical resonator. The distance between the two waveguides is almost negligible for the ease of coupling among the two waveguides.

The proposed Elliptical resonator is a two-dimensional (2D) model. The geometry for the elliptical resonator consists of a rectangle and ellipse which further have metallic rods that runs along the length of the proposed structure. Here, the refractive index of silica is taken as 1.5.

The core represents two different materials – Silicon Carbide and Silicon Nitride which have refractive index = 2.6 and 2.1 respectively. The geometry is characterized by a specific set of parameters that are tabulated below:

Name	**Expression**	**Value**	**Description**
w_core	0.2[μm]	2E-7 m	Core Width
w_cladding	10*w_core+0.0000001	2.1E-6 m	Cladding Width
n_core	2.5	2.5	Core Refractive Index
n_clad	1.5	1.5	Cladding Refractive Index
W_1	1.55[μm]	1.55E-6 m	Wavelength
Dx	3.5833*w_core	7.1666E-7 m	Separation between waveguides
r_o	4*wl	6.2E-6 m	Radius of curvature
f_o	c_const/wl	1.9341E14 1/s	Frequency
A	r_o+w_clad/2*a	1E-6 (r_o+a) m	Semi – Major Axis

Table 3.1 List of parameters required for designing and simulation of the sensor

For designing of resonator, the **geometry primitives** of the ellipse have semi-minor axis= r_o+w_clad/2*1.1 and semi-major axis= r_o+w_clad/2*3 is designed along with 3 different layers having particular thickness and further the inner portion of ellipse is removed to prepare a hollow ellipse.

Layer Name	Thickness (m)
Layer 1	(w_clad-w_core)/2
Layer 2	w_core
Layer 3	(w_clad-w_core)/2

Table 3.2 Description of thickness of three layers required for ellipse

A rectangle having width= w_clad and height= $2*r_o+w\_clad*3$ with centre point at $-(r_o+dx)$.Also, layers to the left and right are selected having defined value instead of the bottom layer.

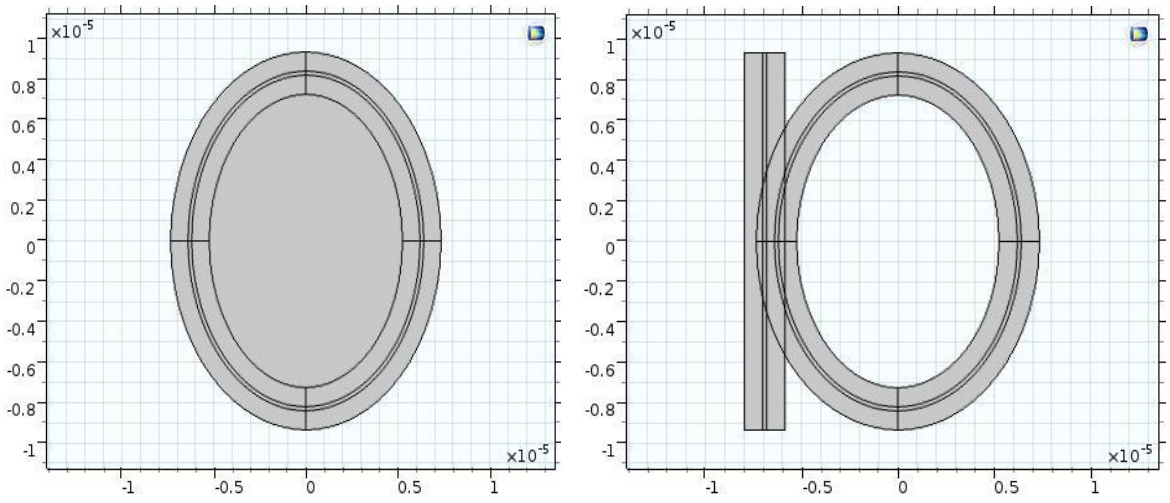

(a) (b)

Figure 3.1 (a) Elliptical Shaped Waveguide, (b) Rectangular Shaped Waveguide

For making the connectivity among the two shapes we use union operator from Booleans and Partitions section to remove the unwanted boundaries. Further to avoid the overlapping portions, certain entities are deleted from the rectangle. Here certain values like refractive index, physics are kept constant but width of semi minor axis, wavelength range, frequency are varied for obtaining the graph.

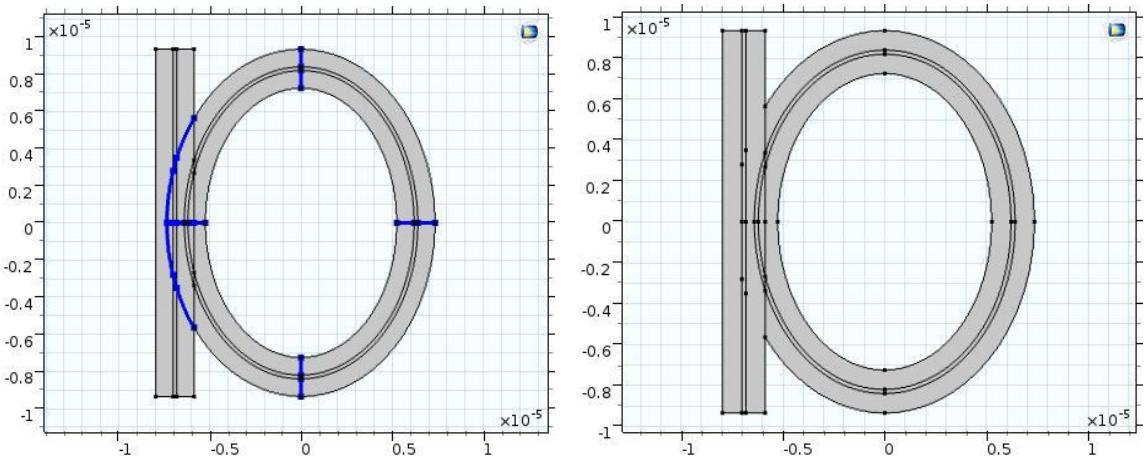

(a) (b)

Figure 3.2 (a) Unwanted Boundaries deleted, (b) Complete Optical Resonator Design

The **materials** employed for cladding part of ellipse and rectangle located in the material contents section have refractive index= n_clad and n_core for the metal rods inserted at the core portion of the resonator. Here we have taken silica for the cladding part due to its numerous advantages like found in abundance in the earth and easily available, fabricated easily, lower energy gap, lower current leakage. Therefore silica is preferred.

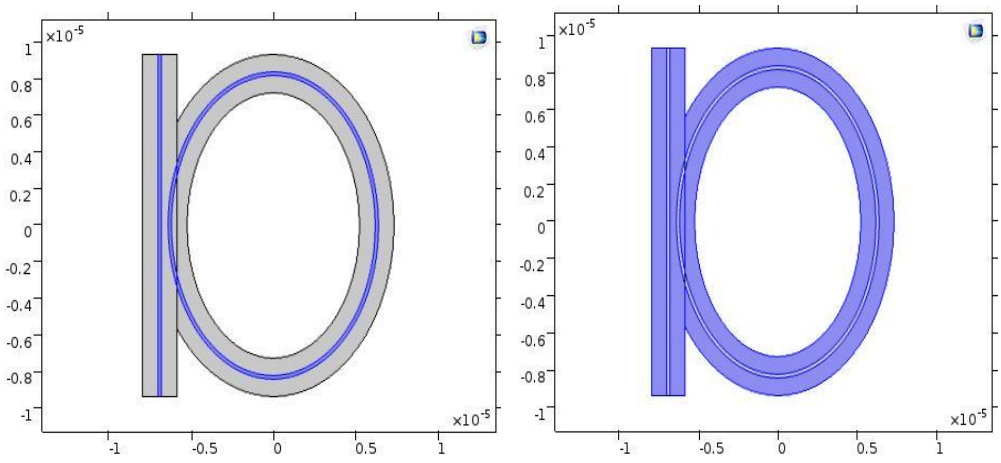

(a) (b)

Figure 3.3 (a) Core consisting of metallic rods, (b) Cladding consisting of Silica

Further, from the physics interface- **Electromagnetic Waves, Beam Envelopes (embe)** is selected to handle the propagation over distances that are many wavelengths long. Since the wave propagates in essentially one direction along the straight waveguide and along the

waveguide ellipse, the unidirectional formulation is used. This assumes that the electric field for the wave can be written as:-

$$E=\mathbf{E_1}\exp(-j\phi)$$

Where $\mathbf{E}_1$ is a slowly varying field envelope function and ϕ is an approximation of the propagation phase for the wave.

Addition of definitions is done for specification of phase in the two waveguide domains that is straight and ring waveguide, value is defined along the y-direction as shown in Table:-

Name	**Expression**	**Waveguide Type**
Phi	ewbe.beta_1*y	Straight waveguide
Phi	ewbe.beta_1*r_o*atan2(-y,x)	Elliptical waveguide

Table 3.3 Phase values for Straight and elliptical waveguides

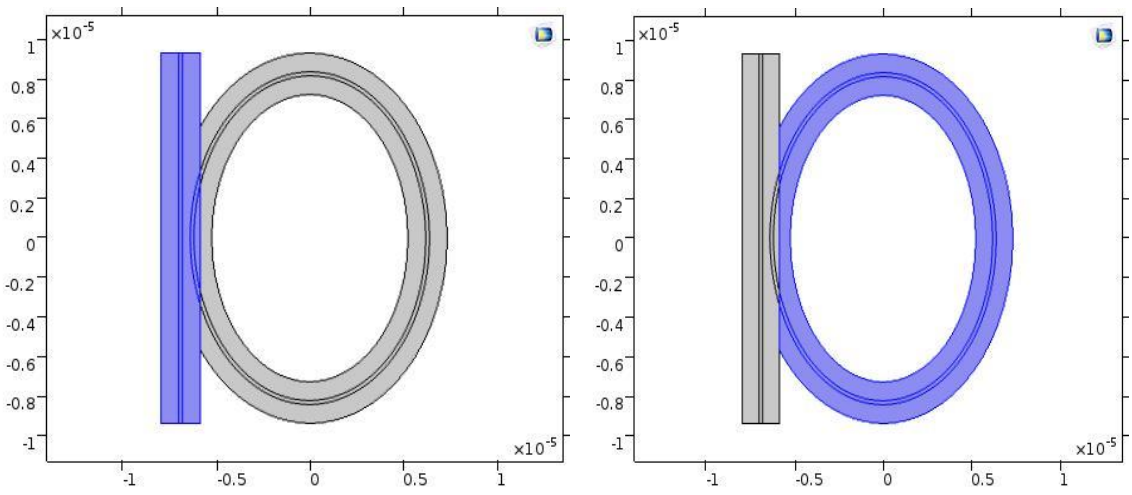

(a) (b)

Figure 3.4 (a) Rectangular Waveguide Phase, (b) Elliptical Waveguide Phase

Here phase that is ‘phi’ and direction (unidirectional) of the light propagation is defined. In addition to this, from the physics toolbar **port conditions** are chosen for exciting the model with an EM wave at input and output ports like waveguide port is excited at input port but off at output port.

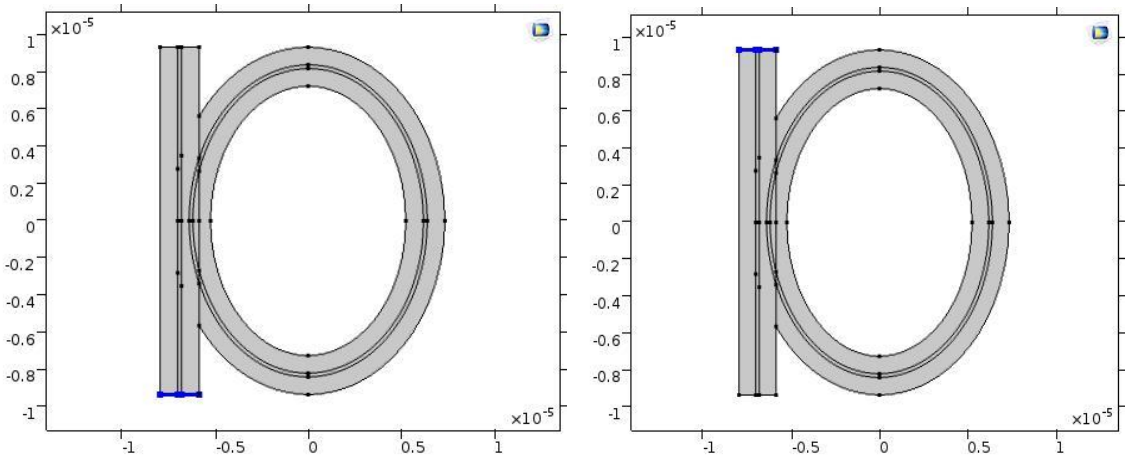

(a) (b)

Figure 3.5 (a) Input Port 1 (b) Output Port 2

For avoiding the reflectance, scattering boundary condition is used at elliptical portion and remaining parts of rectangle.

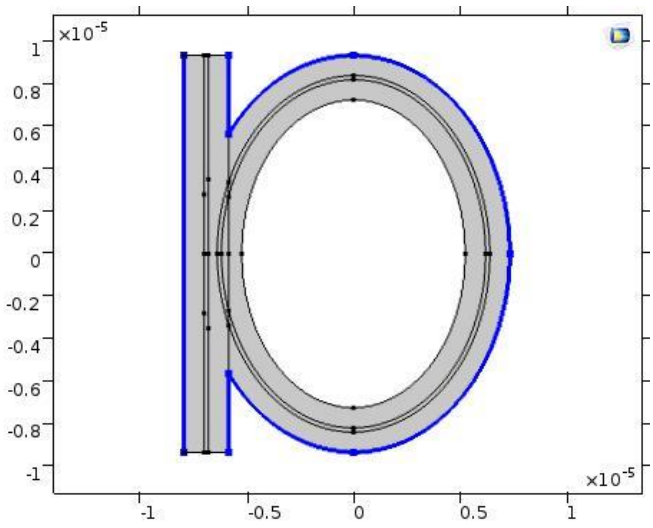

Figure 3.6 Scattering Boundaries

To handle the phase discontinuity and thereby the discontinuity in the field envelope, $\mathbf{E}_1$, a Field continuity boundary condition is used at the boundary between the straight waveguide and the elliptical waveguide. This boundary condition ensures that the tangential components of the electric and the magnetic fields are continuous at the boundary, despite the phase jump.

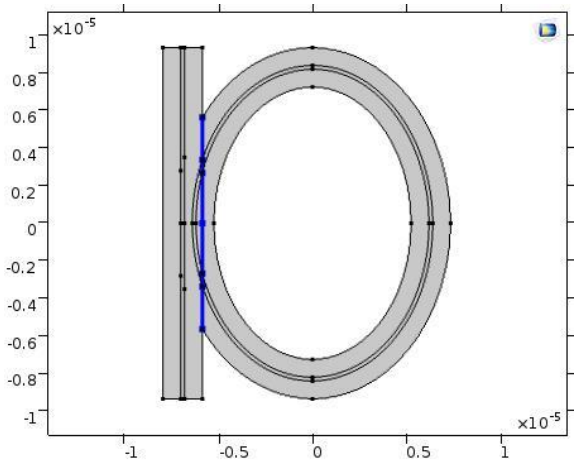

Figure 3.7 Field Continuity Boundaries

The transmitted fields are related to the incident fields through the matrix-vector relation:-

$$\begin{matrix} E_{t1} \\ E_{t2} \end{matrix} = \begin{bmatrix} t & k \\ -k^* & t^* \end{bmatrix} \begin{matrix} E_{i1} \\ E_{i2} \end{matrix}$$

The matrix elements defined above, assures that the total input power equals the total output power. We assumed that the coupling coefficients are interrelated by the following equation:-

$$t^2 + k^2 = 1$$

Further as the wave propagates through the ellipse, we get the following relation:-

$$E_{i2} = E_{t2}\text{Lexp (-j}\phi\text{)}$$

Where *L* is the loss coefficient for the propagation around the ellipse and ϕ is the accumulated phase.

Here the transmission coefficient is separated into the transmission loss (t) and the corresponding phaseϕ_t.

$$\text{t= (t)}e^{-j\phi_t}$$

Notice, that on resonance, when ϕ-ϕ_t is an integer number times 2π, and when |*t*| = *L*, the transmitted field is zero. The condition that |*t*| = *L* is called critical coupling. Thus, when the coupler's transmission loss balances the loss for the wave propagating around the elliptical waveguide we get the optimum condition for a band stop filter, a notch filter.

We use **meshing** because as we refine the mesh, the solution will become more accurate. This helps in obtaining more precise results so here customized mesh is employed consisting of maximum element size to be w_clad/2.

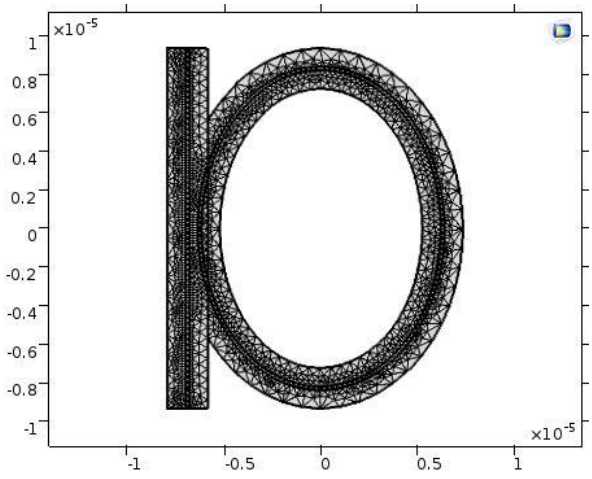

Figure 3.8 Meshed Design

In the final to achieve the desired output study is done by using Boundary Mode Analysis where Mode analysis frequency is f_o and modes are searched around the refractive index of core. This study is applied at both port 1 and 2. Latter Parametric sweep is set in the frequency domain for computing the results in a particular desired range like it is run for wavelength from 1.54µm to 1.57µm consisting of 25 values in between. Finally, the study is computed.

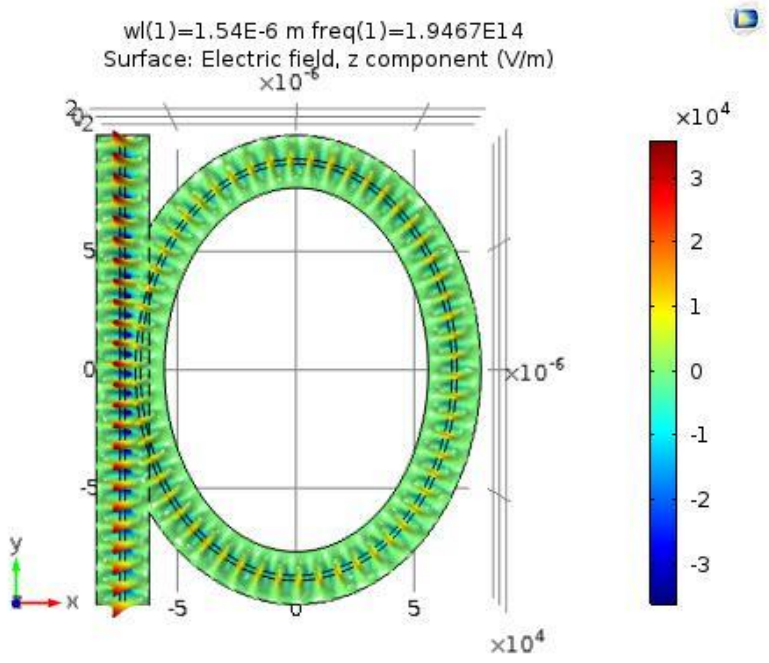

Figure 3.9 The out-of-plane component of the electric field for the resonant wavelength

For obtaining the graphs, in the Electric Field (ewbe) toolbar expression for light propagation that is 'ewbe.Ez' is given and viewed in XY plane. For plotting the graph between transmission and wavelength in 2D Plot Group, parametric value 1.5603E-6 is chosen and plotted. Further, from the Home toolbar 1D plot group is added for graph plotting. A desired study that is Study1/Parametric Solutions1 (sol4) is chosen in the data set. In the graph, Transmission along y-axis and Wavelength along x-axis by using Transmittance equation = abs (ewbe.S21) ^2, the final result is obtained.

3.4 RESULTS AND ANALYSIS

Finally, the results for optical resonator reveals that when an elliptical resonator is designed instead of ring resonator only a small fraction of the incident wave E_{i1} is coupled over the ellipse when we transmitted the field in the straight waveguide as a major part of it travels in the straight waveguide itself. In the similar manner, most of the light wave couples across the elliptical waveguide when fields are transmitted in the elliptical waveguide in contrast to a fraction of wave which continues to couple over the rectangular waveguide.

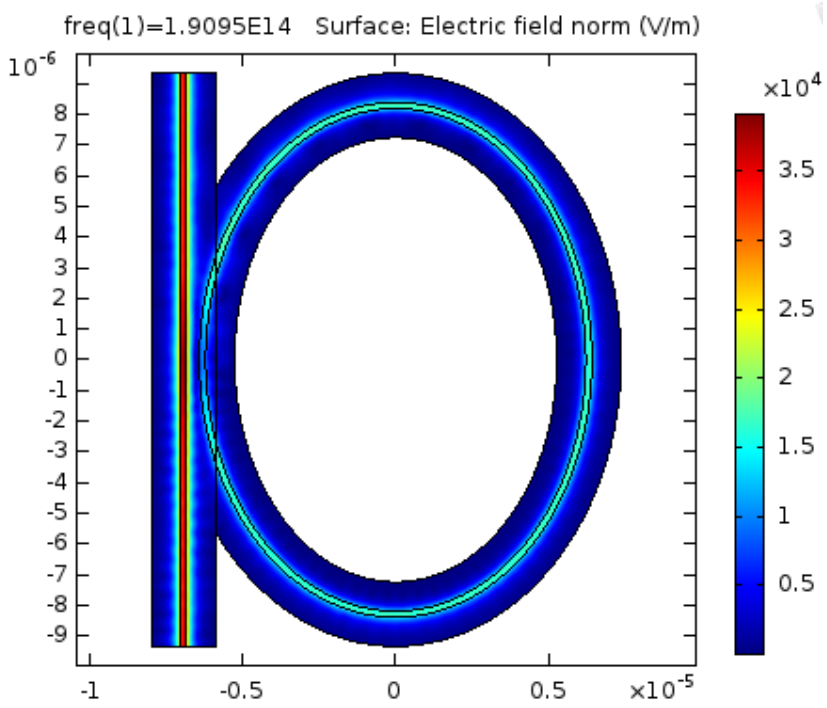

Figure 3.10 Plot of the pre-defined phase approximation. Notice that the phase jump at y = 0 in the cladding of the left part of the ring waveguide is neglected, as the light is mainly confined to the waveguide core.

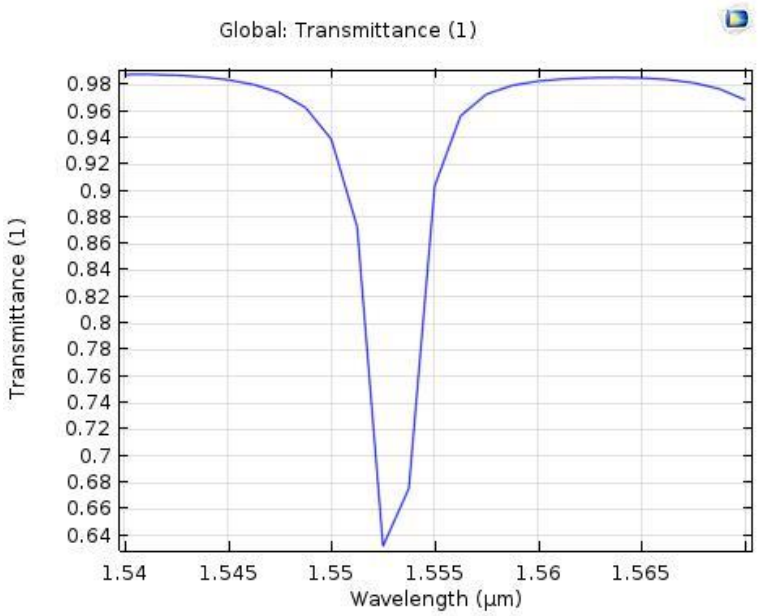

Figure 3.11 Transmittance spectrums for the optical ring resonator

The above figure depicts transmission curve for ring resonator where a dip is observed in the range of 1.55 to 1.555μm and an improvement is made in this shift by using an elliptical resonator instead of ring resonator.

It is evident that outgoing field in the rectangular waveguide will be equal to zero when there is proper coupling like field going in the rectangular waveguide and the wave coming outward from the ellipse are out of phase. Therefore, when a balance is maintained between the loss caused due to transmission of coupler and wave propagation around the elliptical waveguide we achieve the optimal condition for the desired filter.

Further, the transmission versus wavelength graph depicts improved value when ellipse shaped resonator is employed instead of ring waveguide for varying values of minor axis that is having dimension of 4μm, 3.5μm and 3μm respectively along with major axis fixed at r_o+w_clad/2*a by adding different materials in the core - Silicon Carbide (n= 2.6) and Silicon Nitride (n= 2.1) respectively.

It is analysed that as the dimensions of the minor axis increase, sensitivity follows an increasing trend for both materials which means sensitivity is directly proportional to an escalation in the dimensions of the ellipse.

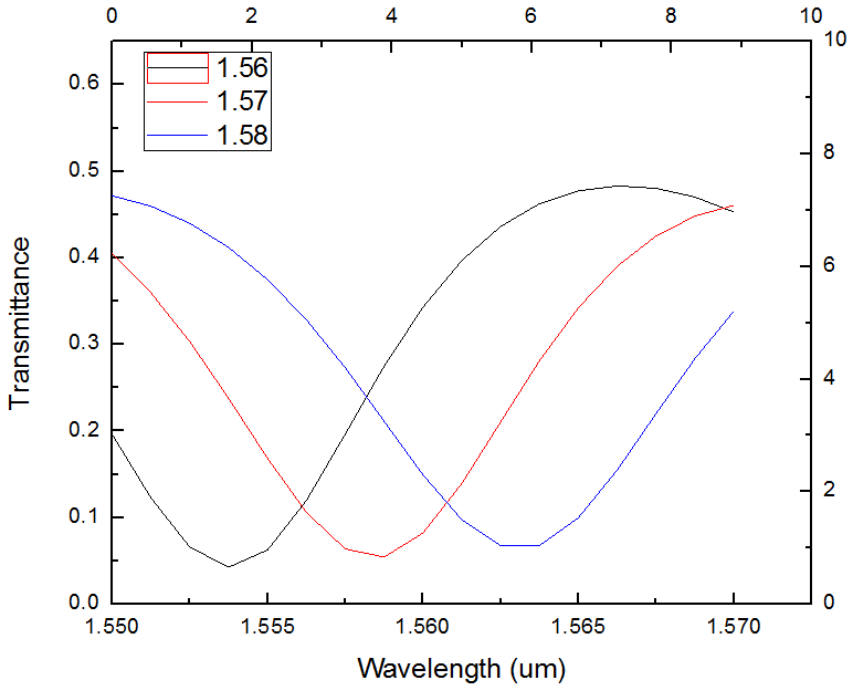
1.56
1.57
1.58
Transmittance
Wavelength (um)
0.0
0.1
0.2
0.3
0.4
0.5
0.6
1.550
1.555
1.560
1.565
1.570
0
2
4
6
8
10

(a)

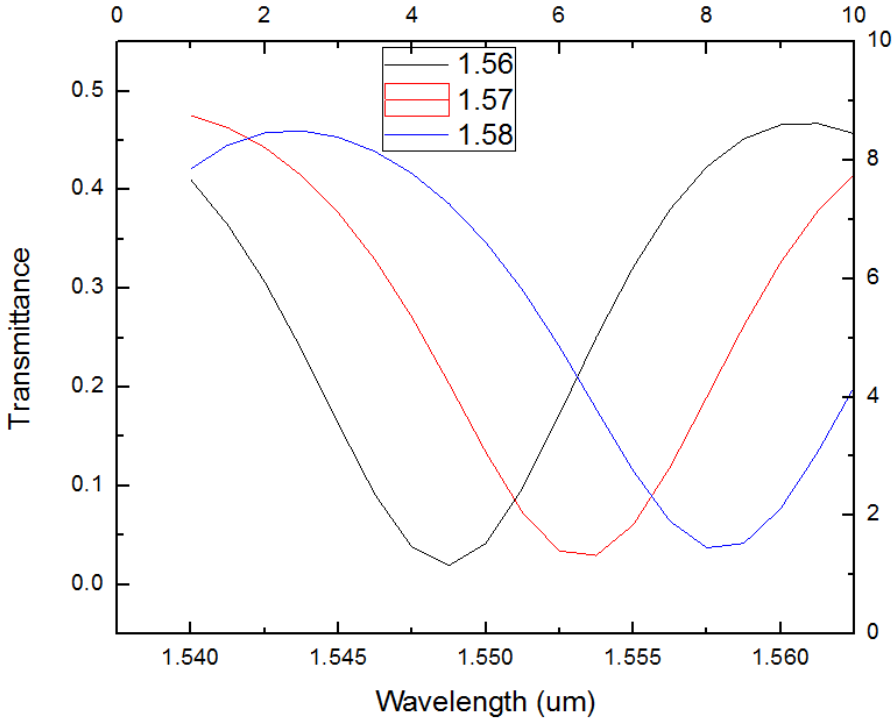
1.56
1.57
1.58
Transmittance
Wavelength (um)
0.0
0.1
0.2
0.3
0.4
0.5
1.540
1.545
1.550
1.555
1.560
0
2
4
6
8
10

(b)

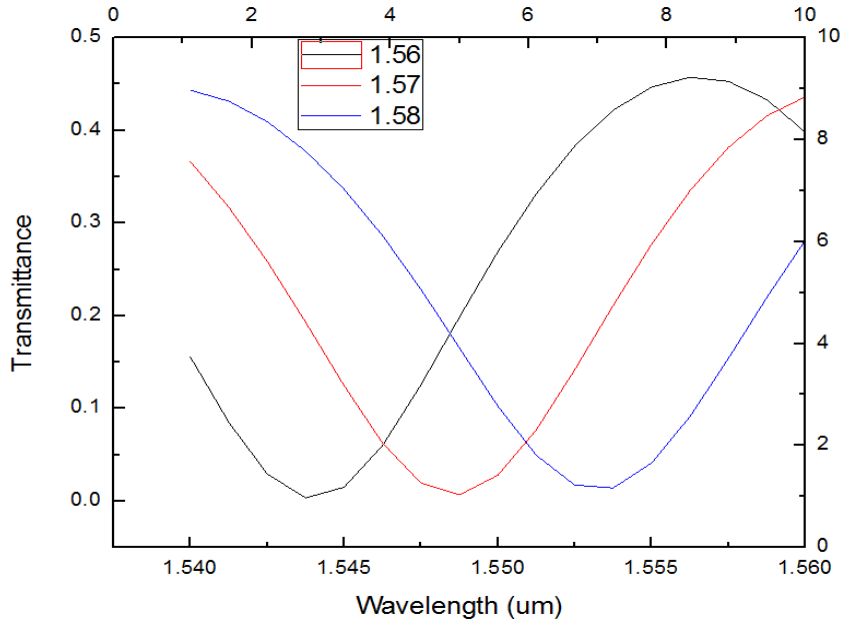

(c)

Figure 3.12 Output Transmission Spectrum at different refractive indexes for semi minor axis: - (a) r_o+w_clad/2*3 (b) r_o+w_clad/2*3.5 (c) r_o+w_clad/2*4 having core = Silicon Carbide

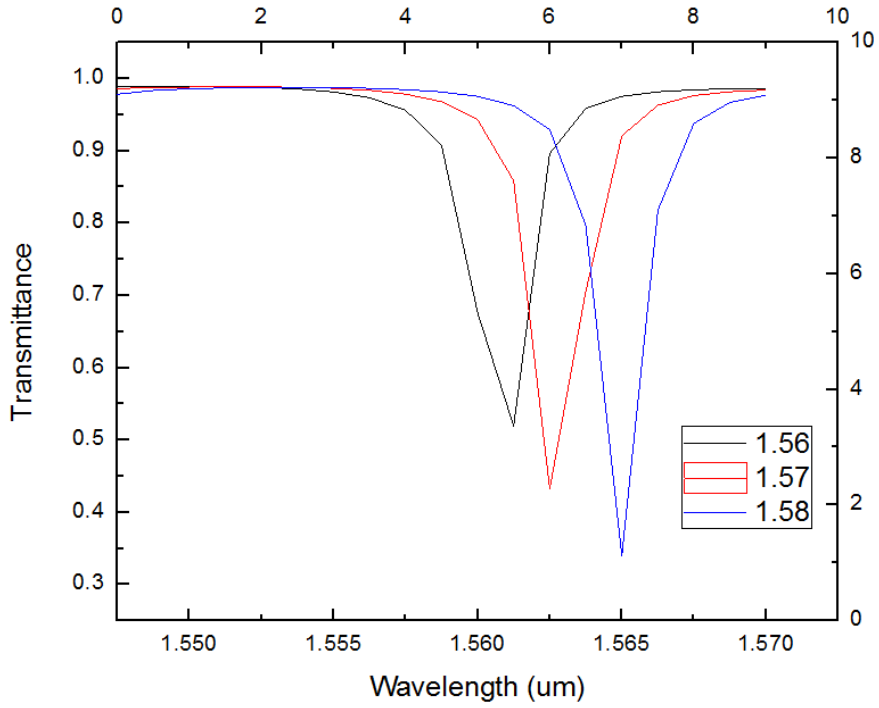

(a)

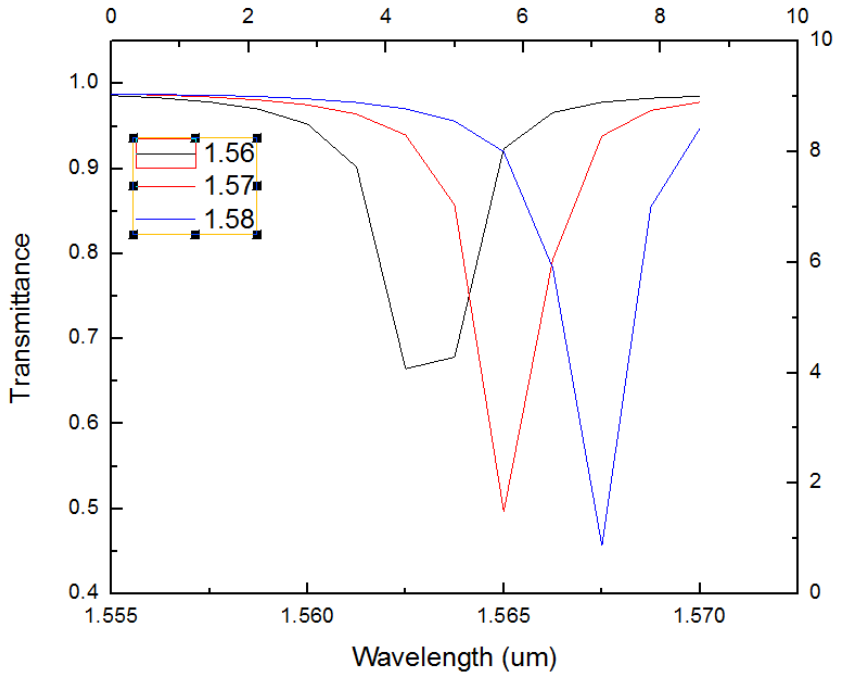

(b)

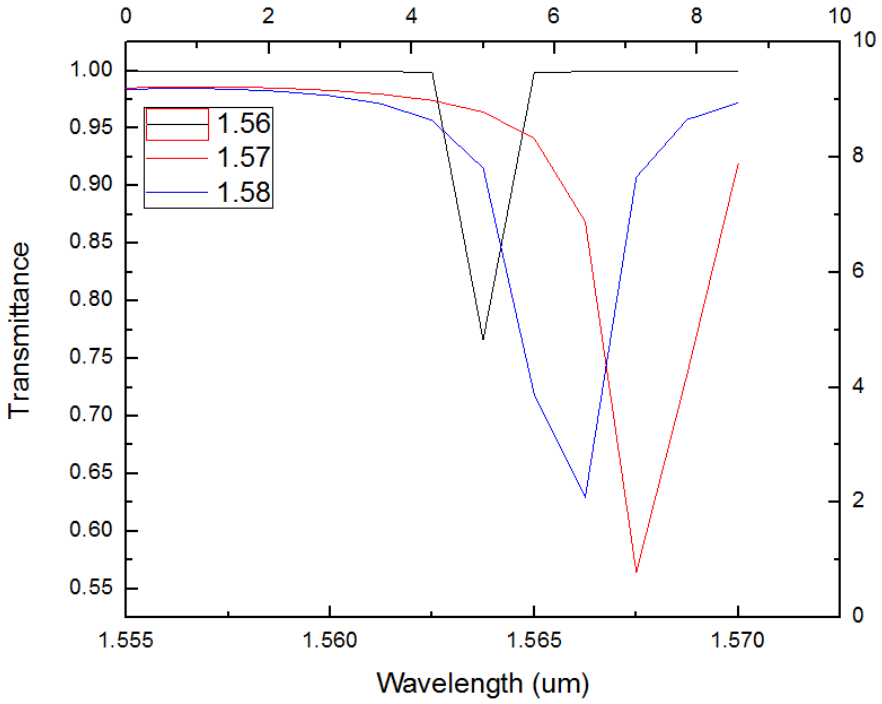

(c)

Figure 3.13 Output Transmission Spectrum at different refractive indexes for semi minor axis: - (a) r_o+w_clad/2*3 (b) r_o+w_clad/2*3.5 (c) r_o+w_clad/2*4 having core = Silicon Nitride

As explained above, variation in the materials employed leads to increase in light confinement. Because of this, there is variation in the refractive index of core which further leads to an increase in the sensitivity with the increase in the minor axis. The sensitivity increases from 187.5nm/RIU to 312.5nm/RIU for Silicon Carbide and from 437nm/RIU to 500nm/RIU for Silicon Nitride as shown in Figure 3.12 and 3.13 respectively.

It is analysed that there is shifting towards higher wavelengths which is termed as Red Shift and sharp dips are observed for material having higher value of refractive index. There is increase in sensitivity due to change in refractive index value as there is better and effective guiding of light through the waveguide. This leads to an increase in the guiding mode energy. Although the width of major axis, cladding, core remain fixed but there is variation in minor axis. As described in transmission spectrum, there is no effective transmission at greater dimensions as shown in Figure 3.14 and even the electric field norm decreased to 3E4 (V/m) from 3.5E4 (V/m). So we fix the dimensions at 4µm only for further simulations.

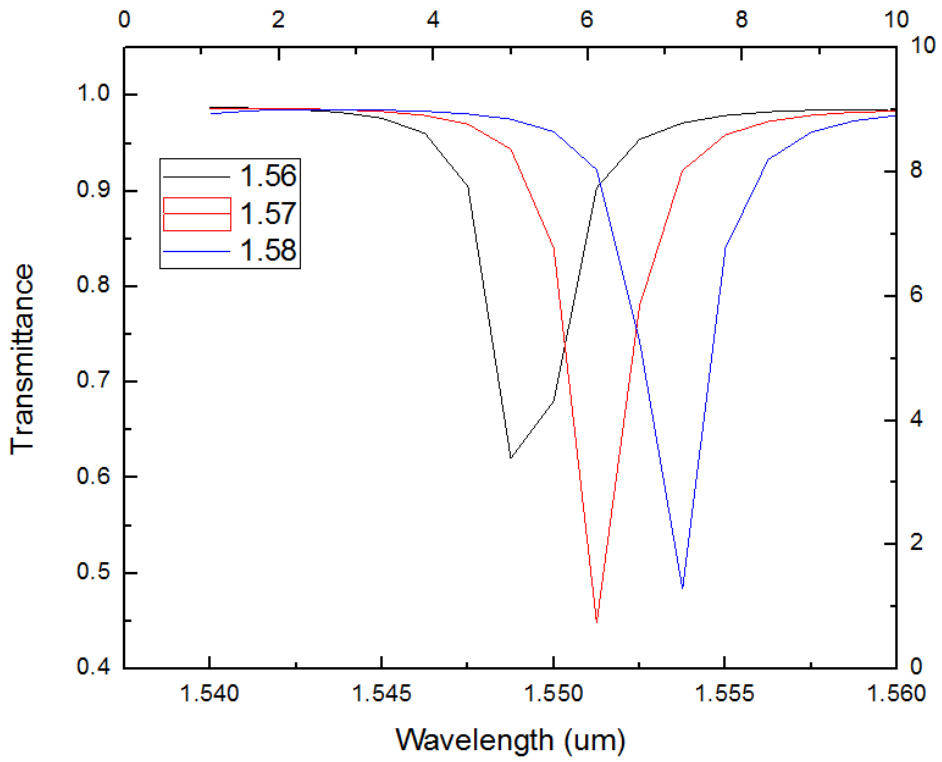

Figure 3.14 Output Transmission Spectrum at different refractive indexes for semi minor axis = r_o+w_clad/2*4.5

It is observed that for appropriate design and to achieve high performance, various aspects need to be taken into account. It is vivid that for sharp resonance that is high quality factor, there is requirement of small resonance wavelength shifts that are important for switching and sensing applications. The quality factor for every device is dependent on the parameters chosen for geometry. As explained above, variation in the geometrical parameters leads to high quality factor. Therefore, here variations are done in the semi minor width which reveal increase in the Q factor as the width is escalated. It is vivid from Figure 3.15 that for both materials that are silicon carbide and silicon nitride, Q factor and width are directly proportional to each other and for a= 3.00μm minimum Q factor was recorded but for a= 4.00μm, the value of Q factor was optimum that is 177×10^3 and 626×10^3 for silicon nitride and silicon carbide respectively. This optimized value is best suited to make photonic crystal based resonators.

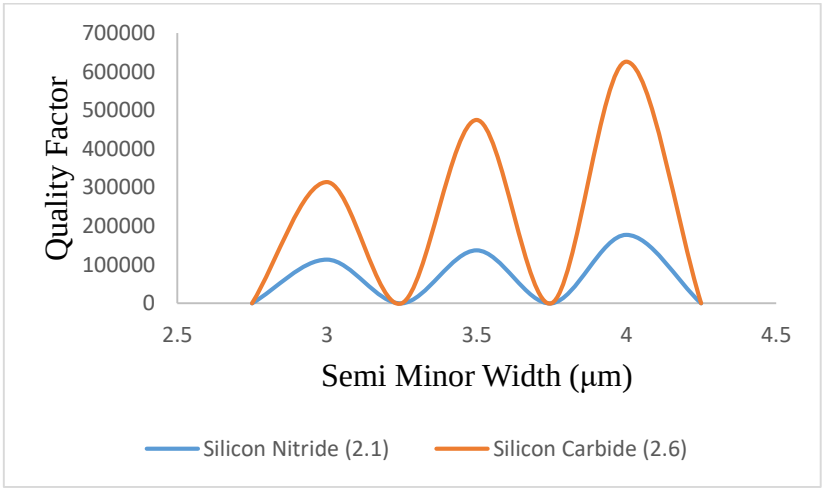

Figure 3.15 Quality Factor vs. Semi Minor Width for different materials

3.5 CONCLUSION

It is concluded that by replacing the ring waveguide by an elliptical waveguide and further insertion of metallic rods in the core of different material which has higher value of refractive index as compared to the cladding part of the optical resonator, we not only achieve high transmission efficiency but even obtain accuracy in coupling of light between the rectangular and elliptical waveguide as the losses are minimized. Even the sensitivity of the resonator increased with variation in refractive index and dimensions where a value of 500nm/RIU was recorded. The Quality Factor having value as high as 626×10^3 was obtained. The Electric Field

norm has increased to 3.5E4 (V/m) for elliptical resonator which was just 1E5 (V/m) in case of a ring resonator.

CHAPTER 4

HIGH SENSING PERFORMANCE USING SELECTIVELY FILLED SOLID CORE PHOTONIC CRYSTAL FIBER WITH GOLD NANOWIRES

4.1 INTRODUCTION

The Photonic Crystal Fiber (PCF) is also called microstructure fiber [73] which is a type of fiber having a structure consisting of 2-D photonic crystals. In the recent days, PCF has engrossed extensive attraction as it comprises of a simple periodical array made of air holes along the whole cladding portion of the fiber. The designs made in PCF are preferred over conventional optical designs because of many beneficial aspects it has as compared to it like mode propagation, controllable birefringence, high confinement, low non-linearity etc. [74]. The cross sectional part consists of complex value of distribution of refractive index where the holes are arranged in diverse form as per the requirement. The size of holes is decided in accordance with the value of wavelength so that the light can be confined at the desired position. Furthermore, the presence of air holes even helps to insert some desirable contents which can further be beneficial for transmission and confinement of light [75]. Recently, many sensors based on PCF are established which can measure temperature [76-80], vibration [81], strain [82], refractive index (RI) [83], [84], twist [85], magnetic fields [86],gas absorption [87], optical sensing [88] and many more which are extensively utilized for various applications like in field of chemicals, bio sensing and physical. Peng *et al.* designed a temperature sensor which was a PCF coated selectively and had sensitivity about 720 pm/°C [89]. Later, Liu *et al.* proposed a similar sensor which consisted of a PCF coating with a gold film of nanosize. He analyzed that coupling can occur with ease if air holes from the second layer are removed and thus achieved approximately −2.15 nm/°C sensitivity [90], whereas all of these employed simulations numerically and furthermore coating was one of the problem being faced when experimental results were derived. To overcome these coating enigmas, many scholars presented sensors filled of metallic nanosize particles. Later, a researcher,[91] Csaki *et al.* proposed a new design comprising of metallic nanosize particles layer technique by employing self-assembled single layer method and obtained Sensitivity as 78 nm/RIU. Lu et al. also proposed a temperature based sensor having silver nanowires and depicted sensitivity [92] but,

it was not an easy task to function with selective filling of nanowires [93] and further it even decreased mechanical stability [94] that confined many of its applications [95].

In this paper, a PCF of hexagonal shape is designed filled with gold nanowires which is analysed theoretically and demonstrated. The software employed is COMSOL Multiphysics and the simulations depicted wavelength resonances are shifting towards higher wavelengths that is red shift is achieved when we varied the value of lattice constant. A considerable progress is made as compared to the previous works done in this field. Moreover, insertion of gold wires has improved the accuracy significantly. The results revealed that lattice constant variations influence the attenuation leading to the fundamental mode effective index.

4.2. SENSOR DESIGN

The geometry based on 2-D photonic crystals consists comprises of seven layers of air holes along with gold nanowires inserted in the innermost layer of air holes. There is specific set of parameters employed for designing the proposed PCF structure.

NAME	EXPRESSION	VALUE	DESCRIPTION
A	6.5[µm]	6.5E*6 m	Lattice Constant
r_c	3[µm]	3E-6 m	Diameter of air holes
dh	0.090[µm]	9E-8 m	Diameter of gold nanowires
w	1.55[µm]	1.55 E-6 m	Wavelength
f	c_const/w	1.9341E14 1/s	Frequency
dclad	125[µm]	1.25E-4 m	Diameter of the Fiber
dcore	10[µm]	1E-5 m	Diameter of the Core

dampz	real(-w)	-1.55E-6 m	Attenuation Constant
dampzdB	20*log10(exp(1))*dampz	-1.3463E-5 m	Attenuation constant in dB

Table 4.1 List of parameters required for designing and simulation of the sensor

The primitives employed for designing of PCF based sensor is circular shaped air holes having diameter = r_c. Depending on the distance between the holes, waves within a specific frequency range are reflected instead of propagating through the crystal. Therefore, the lattice constant =6.5µm is defined as the distance between the two consecutive centres of air holes. The diameter of the gold nanowires = dh whose average length is 30µm. A circle of radius $r_c/2$ is drawn.

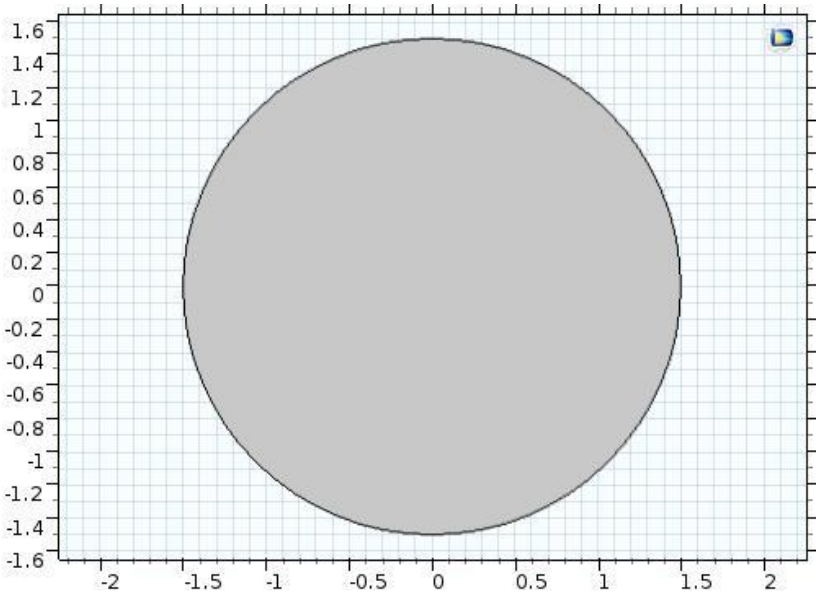

Figure 4.1 Circular air hole with radius = r_c

A linear array of size 7 with a lattice distance of 6.5µm is drawn along both negative and positive X-axis.

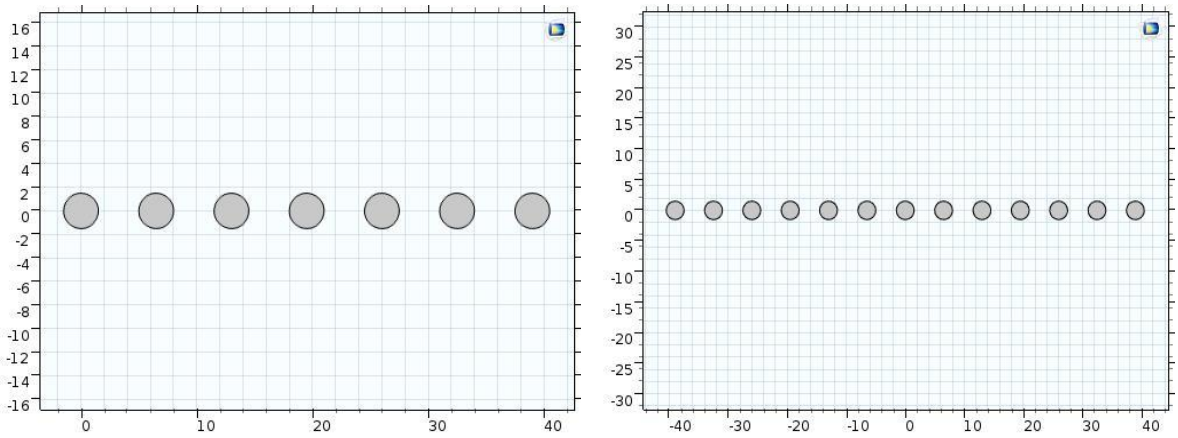

(a) (b)

Figure 4.2 (a) Linear array of size 7 along positive x-axis, (b) Linear array of size 7 along negative x- axis

Further a replica of air holes is made having linear array size 7 and displaced by a/2µm and a*sqrt (1.5)*0.7 along X-axis and Y-axis respectively. As per the requirement, the undesired entities (air holes) are removed along with the centre hole.

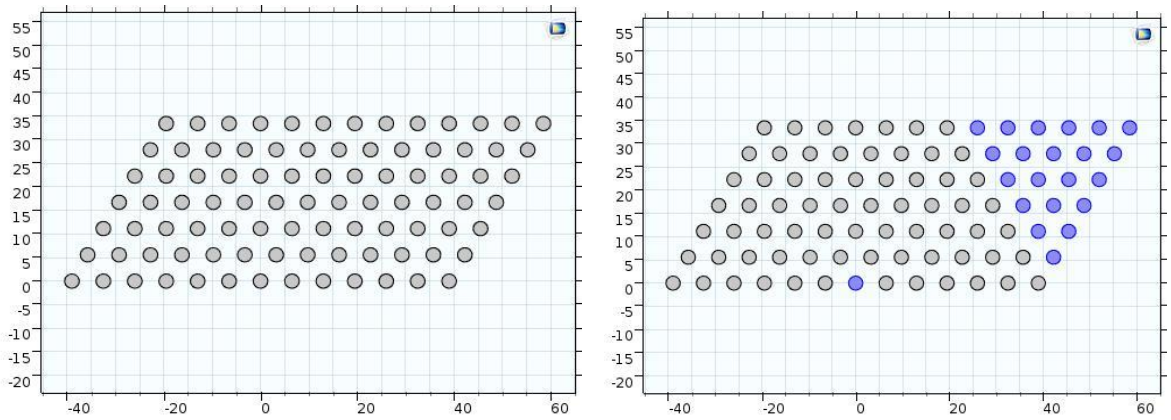

(a) (b)

Figure 4.3 (a) Array consisting of seven layers along positive y-axis, (b) Entities to be deleted to form hexagonal PCF

For obtaining the hexagonal shape, a mirror image is taken by considering a normal vector to line of reflection that is Y-axis by keeping the input objects as well. Finally, a circle enclosing the hexagonal shaped PCF is drawn having radius multiple of lattice constant and a layer of thickness 2µm.

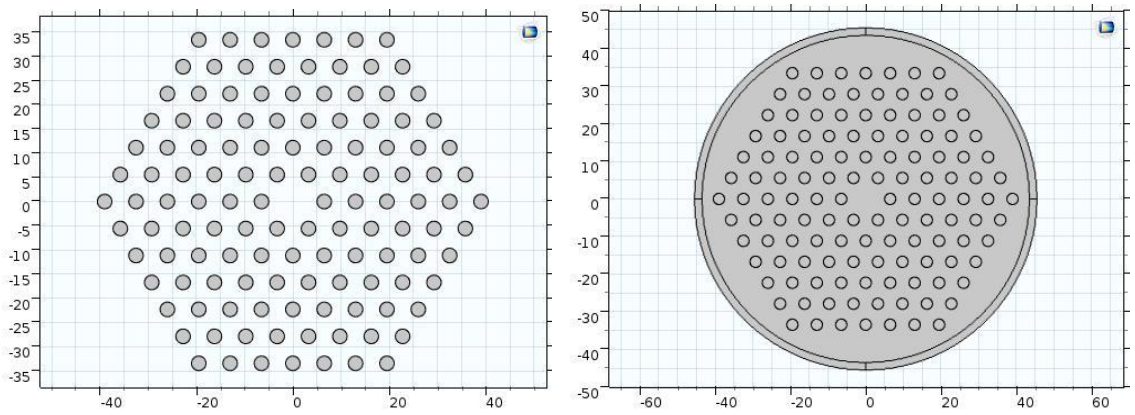

(a) (b)

Figure 4.4 (a) Mirrored Image for design, (b) Complete design of Hexagonal shaped PCF structure

The material employed for cladding part of PCF is air in the holes and silica in the background and even in the core portion silica is present which has refractive index value= 1.45. Here we have taken silica for the cladding part due to its numerous advantages like found in abundance in the earth and easily available, fabricated easily, lower energy gap, lower current leakage. Therefore silica is preferred.

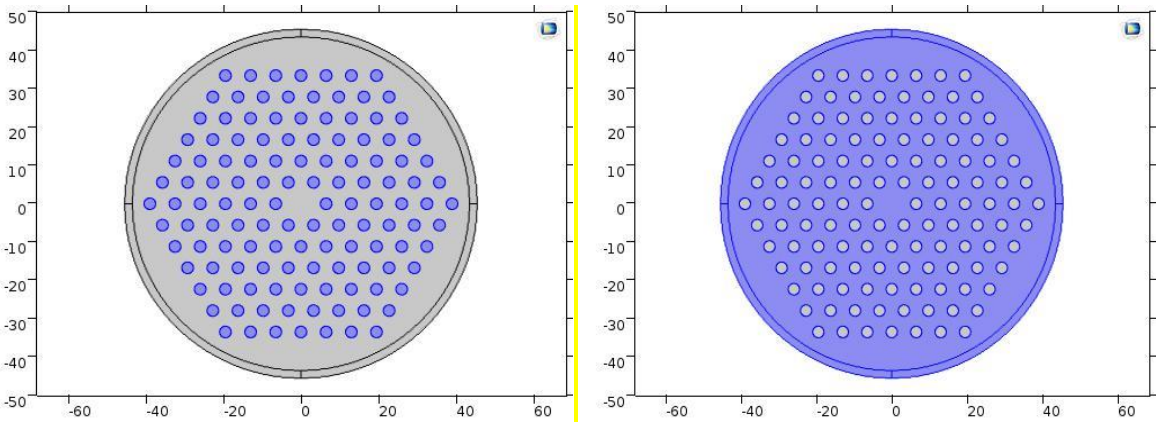

(a) (b)

Figure 4.5 (a) Holes selected for defining air as material, (b) Cladding portion selected for defining silica as material

Frequency Domain is used for generating stationary equations that can be used for frequency sweeps which corresponds to a stationary parametric solver that is present to linearize the equations. The frequency domain formulation uses the following inhomogeneous Helmholtz equation:-

$$\nabla.\left(\frac{1}{\rho_c}\left(\Delta\rho - q_d\right)\right) - \frac{\omega^2}{\rho_c}\rho = Q_m$$

In this equation, $p = p$ (**x**,ω). With this formulation compute the frequency response with a parametric sweep over a frequency range using a harmonic load. When there is damping, $\rho_c$and c_c are complex-valued quantities.

Further, from the physics interface- **Electromagnetic Waves, Frequency Domain (emw**) is selected to confine the light in the core by employing the study based mode analysis equation as described below:-

$$\nabla \times \mu_r^{-1} (\nabla \times \mathrm{E}) - k_0^2 \left(\in_r - \frac{\sigma j}{\omega\epsilon}\right) = 0$$

$$\lambda = -j\beta - \delta_z$$

$$\mathrm{E}(x, y, z) = \check{\mathrm{E}}(x, y)\, e^{-ik\, z^z}$$

The model for electric displacement field is Refractive Index where relative permeability (μ_r) and electrical conductivity (σ) are taken to be zero and the equation is defined as:-

$$\in_r = (n - ik)^2$$

The outermost layer -Perfectly Matched Layer (PML) of cylindrical type due to circular geometry is employed for absorbing the radiations. It has PML scaling factor = 1 and PML scaling curvature parameter also = 1. The initial values for electric field (V/m) along x, y and z axis are defined equal to zero.

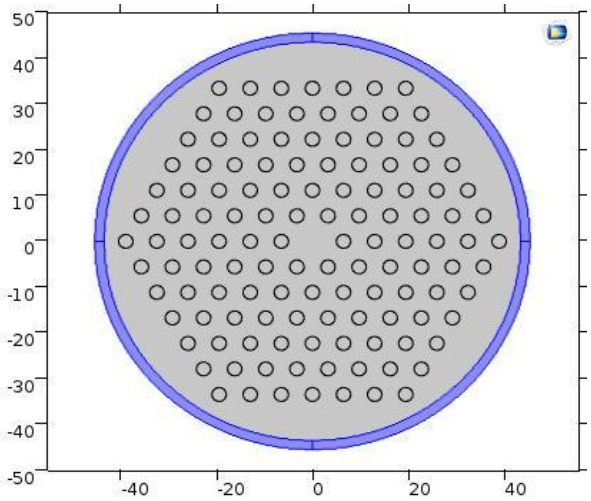

Figure 4.6 Region selected to be defined as PML

The default mesh settings aim for a good resolution of all curved boundaries. In this model, we led to a high number of elements. By relaxing the growth rate and the curvature resolution requirement, we can get a decently accurate solution with fewer elements. So here we have utilized coarse element size for meshing our design.

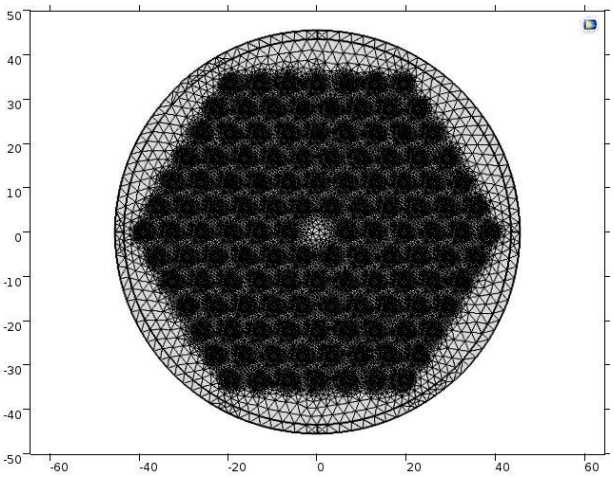

Figure 4.7 Triangular meshed structure

4.3 COMPUTATION OF THE DESIGN

Frequency Domain Modal generates equations for modal analysis in the frequency domain and further corresponds to a modal builder with Study solver positioned at Frequency Domain. In the final to achieve the desired output study is done by using Mode Analysis where default plots and convergence plots are generated. The transformation is performed by selecting effective mode index where mode analysis frequency is ‘f’ Hz and search method employed

for modes is manual where total number of desired modes is 1, modes are searched around a particular value of refractive index which is 1.446. The values of all dependent variables are physics controlled. A parametric sweep allows changing the parameter values through a specified range. The parametric sweep can include multiple independent parameters directly, but we can also add more than one Parametric Sweep node to create nested parametric sweeps. Here parametric sweep is put on wavelength which has range from 1.55 µm to 1.65µm and will provide 10 numbers of values.

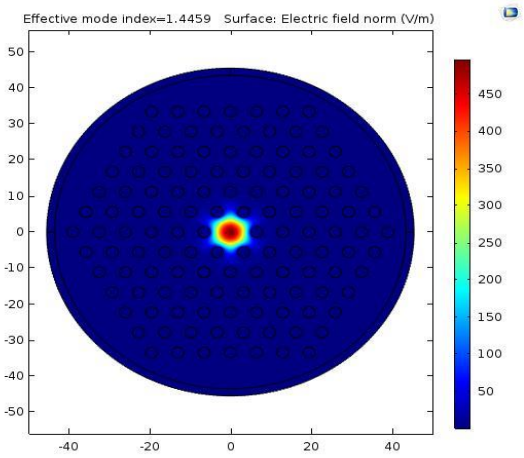

Figure 4.8 The surface plasmon resonance sensor based on PCF regularly filled with three gold nanowires.

For obtaining the **graphs,** in the Electric Field (ewbe) toolbar expression for light confinement that is 'emw.beta' having units rad/m is given and viewed in XY plane. For plotting the graph between transmission and wavelength and attenuation versus wavelength in 2D Plot Group, effective mode index value 1.4459 is chosen and plotted. Further, from the Home toolbar 1D plot group is added for graph plotting. A desired study that is Study1/Parametric Solutions1 (sol4) is chosen in the data set. In the graph, Transmission along y-axis and Wavelength along x-axis by using Transmittance equation = abs (ewbe.S21) ^2 and for Attenuation versus wavelength we took attenuation along y-axis and wavelength along x-axis and achieved the final results.

4.4 MODIFICATIONS

Further to achieve higher accuracy, the design is modified by inserting three gold nanowires in each hole of the innermost layer of air holes with a specific distance between them and

positioned facing the core of the PCF. This modification has a great influence on the transmission and attenuation of the PCF. The design steps required for insertion of nanowires are classified as below:-

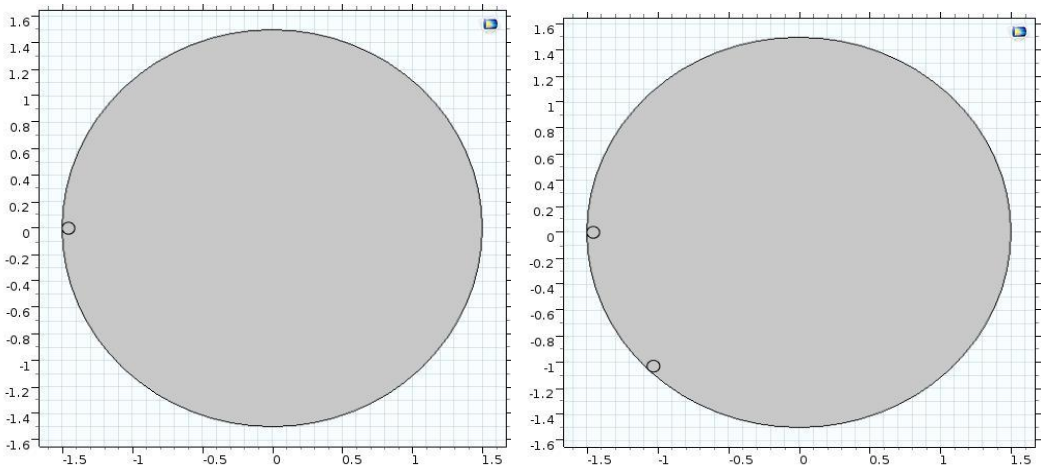

(a) (b)

Figure 4.9 (a) Innermost air holes consisting gold nano wire, (b) Gold nanowire rotated anticlockwise by 45^0

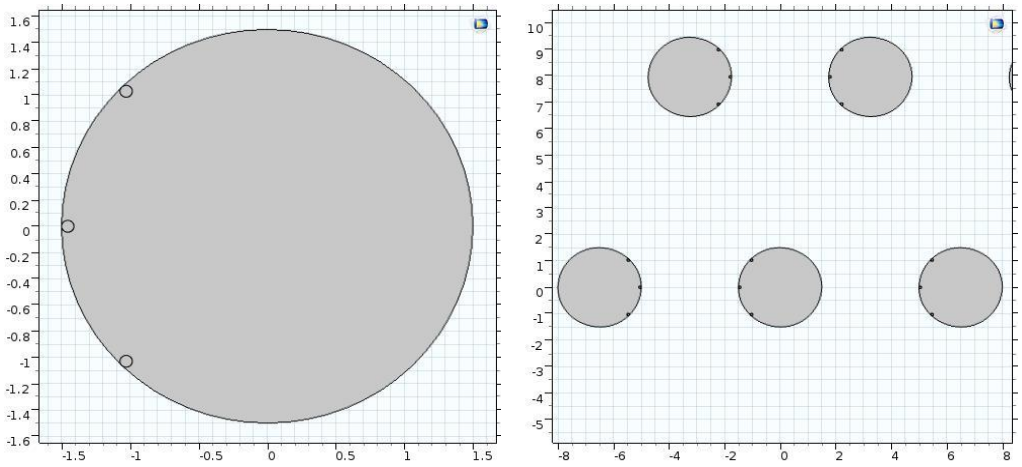

(a) (b)

Figure 4.10(a) Gold nanowire rotated clockwise by $45^{0,}$ (b) Gold nanowires copied in sideward and upper air holes

A circle having radius = dgold/2 and centre at (-1.455, 0) is designed. This circle is copied and rotated to produce duplicate copies at 45^0 and -45^0 respectively. Later, to insert gold nanowires in the innermost layer, we copy already designed nanowires at lattice constant distance along negative x-axis which has centre of rotation at (-6.5, 0). Further, in similar

manner, this circular wire is copied and rotated at 45^0 and -45^0 respectively. To copy along the positive x-axis we displace it by a distance of (-3.59, 0) and rotate with centre of rotation at (6.5, 0). For upper air holes, we displace by same distance but, the centre of rotation is (-3.25, 7.96084) at both 45^0 and -45^0. Further, the gold wires in the lower part of the layer are inserted by taking the mirror image.

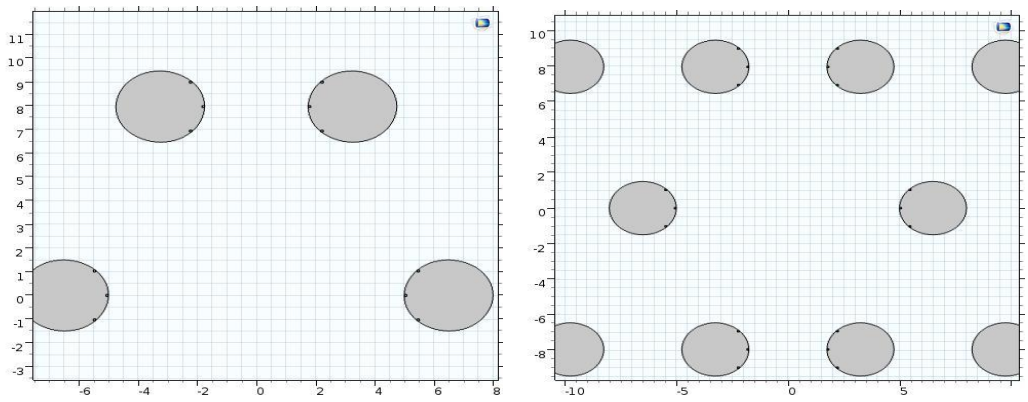

(a) (b)

Figure 4.11 (a) Inner Air hole is deleted, (b) Mirrored image forming a hexagonal shape is formed

4.5 RESULTS

This section illustrates the numerical study of the designed PCF where fundamental mode and some higher order modes are analysed. First we depicted the polarization graph for fundamental mode which included surface plot along x-axis and y-axis respectively as shown in Figure 1.12.

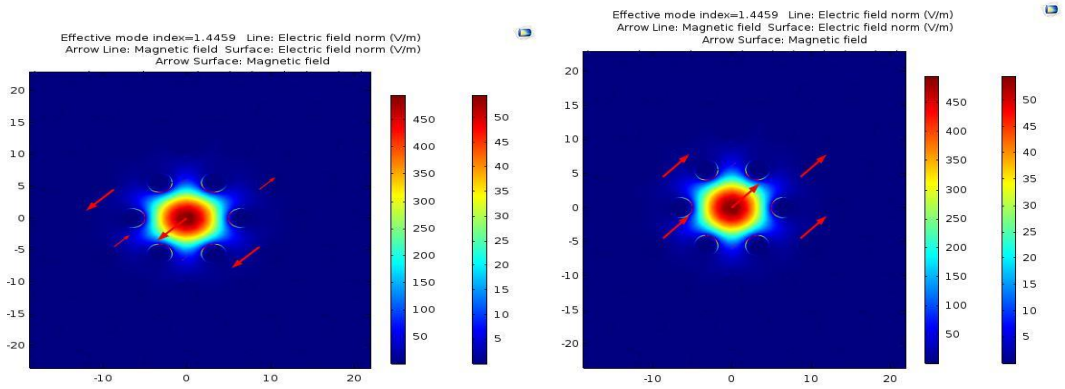

(a) (b)

Figure 4.12 (a) Calculated electric field, (b) magnetic field distribution having Re (N_{eff}) = 1.44594911of the guided-mode at wavelength of the incident light to be 1550nm.

Further, here we have visualized electric field's z-component with the help of height expression by deforming the surface.

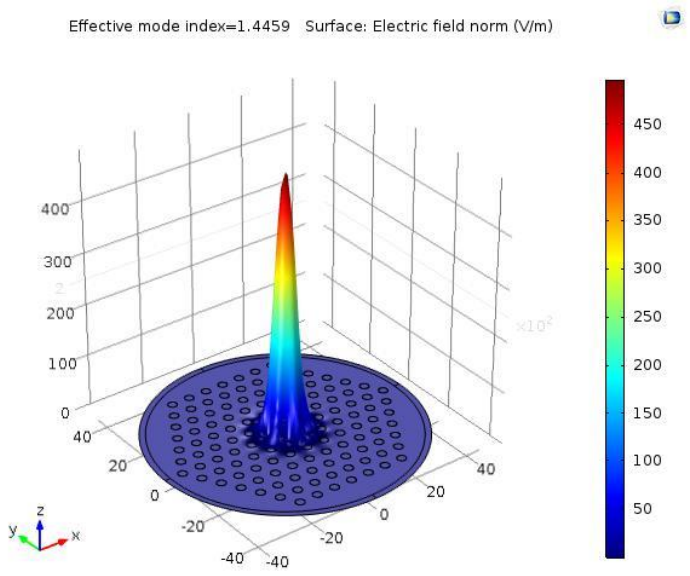

Figure 4.13 Z-component of the electric field with deformed surface

The initial analyses have been performed for evaluating the propagation characteristics within a certain described range of wavelength by assuming the modified design where refractive index and cladding dimensions are kept fixed for all of the proposed PCF calculations. It depicts that constant value keeps on decreasing as the wavelength increases.

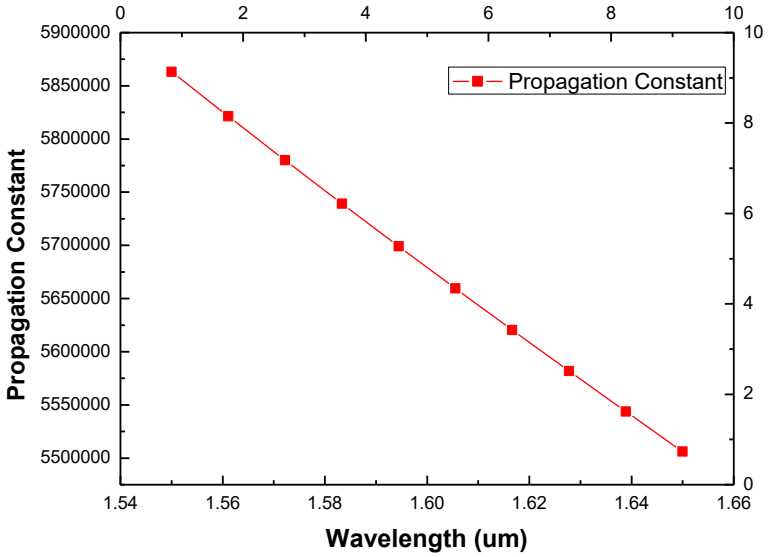

Figure 4.14 The relationship between propagation constant and wavelength

Further, relationship between wavelength and attenuation constant of the fundamental mode of the PCF occupied by three gold nanowires of 900 nm radius each is studied where the graph represents samples with lattice constant 6.5, 6.53, 6.56, respectively. The results are obtained when the expression for attenuation is:-

20*log10 (exp (1))*dampz

Where dampz = real (-w) and damping is considered along z-axis. It represents that the attenuation constant value increases as the lattice constant increase but decreases with increasing value of wavelength as it falls to approximately 1.80E-07 from 2.7E-07 as the wavelength increase by few micrometres as shown in Figure 4.15.

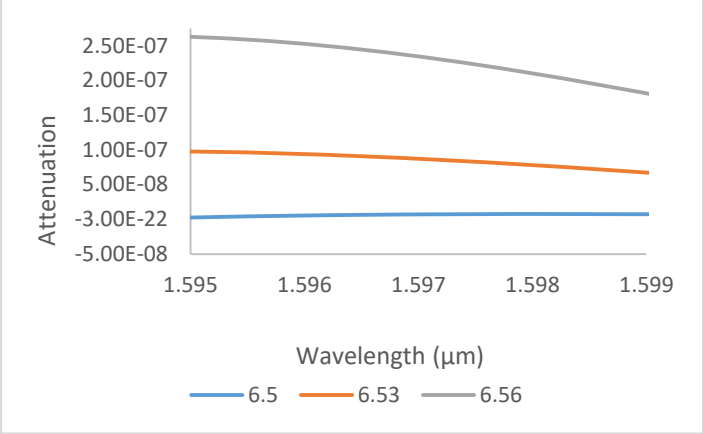

Figure 4.15 The comparison of attenuation constant of the fundamental mode at different values of lattice constant

Effective area examines the optical performance of photonic crystal fiber. The effective area is a significant parameter of non-linearity in PCF. In PCF, the effective area is comparatively low as compared to the standard fibers. Power density factor is also considered as the optical nonlinearity is dependent on it. The effective mode area is given:-

A_{eff} = intop1 (abs (E_z) ^2) ^2/intop1 (abs (E_z) ^4)

Where E is the transverse component of the electric field. It is analysed that the effective area falls an increasing trend with escalation in the wavelength which ranges from 1.57 to 1.64µm as depicted in Figure 4.16. The maximum value of area is 55.15µm^2 that is obtained with lattice constant = 6.56µm.

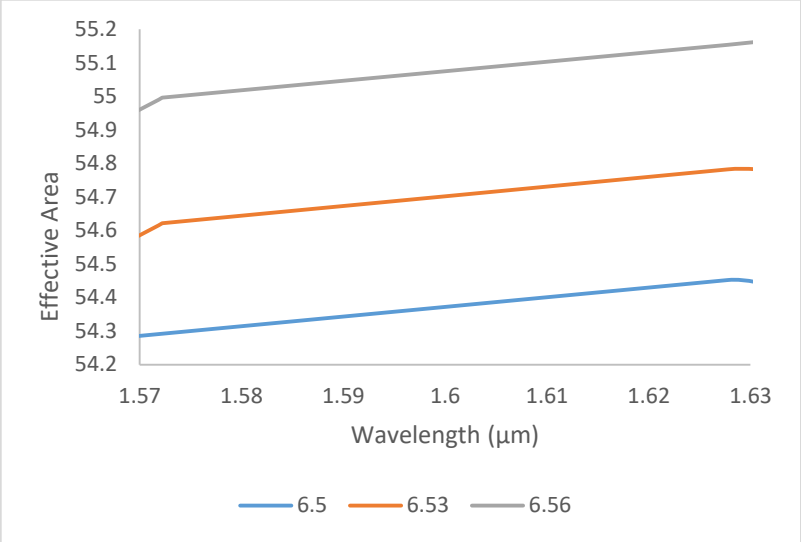

Figure 4.16 Relationship between effective area and shift of the wavelengths at varying lattice constants

Confinement loss is defined as the ability of confining light within the core section and occurs in single material fibers. The increase of air hole rings and size of lattice constants supports the confinement of light in the core section that helps to achieve small losses as compared to PCF which has less number of holes. The confinement loss is defined as:-

$$Lc = 8.686\ k_0 Im\ (ewfd.n_{eff})$$

Where k_0 is wave vector which is emw.beta in this design. At the shorter wavelength the light is less confined in the core part hence the confinement loss is high and it reduces with escalation in value of wavelength as shown in Figure 4.17. There is variation in the confinement loss of photonic crystal fiber as the ratio of air filling in the holes and lattice constant is altered. It is observed that as the lattice constant increases, the losses also surge. Although, the losses lower with rise in the wavelength and reach to zero. Hence, losses can be controlled by altering the lattice constants as per the requirement.

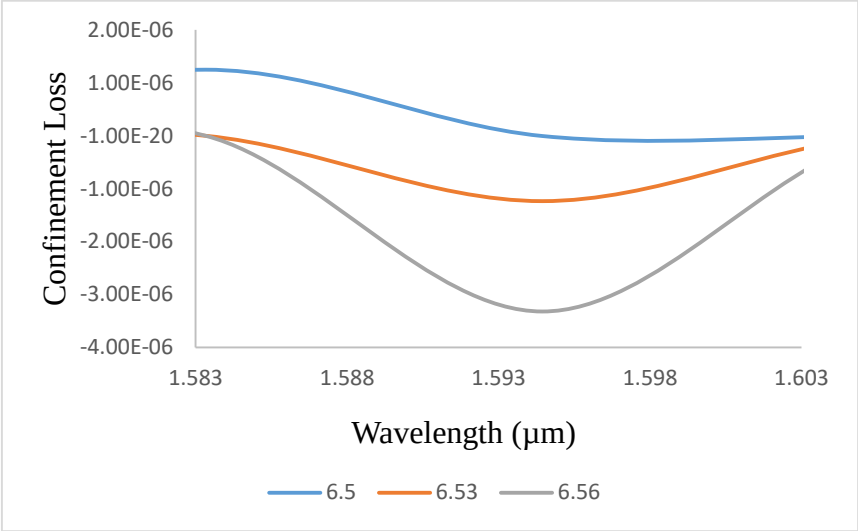

Figure 4.17 The confinement loss of PCF at different wavelengths

The effective refractive index n_{eff} has the similar meaning for light propagation in a waveguide as it has in homogeneous medium where phase constant (β) is equal to the effective index times the vacuum wave number as defined:-

$$\beta = n_{eff} \frac{2\pi}{\lambda}$$

It is known that effective refractive index is dependent not only on the wavelength but also on the mode in which the light is transmitted. Therefore, it is called Effective Mode Index (EMI). The effective index is influenced by the design of the waveguide and values are calculated with numerical simulations. If there is an imaginary part then it means there is gain or loss in the quantity. Figure 4.18 reveals the linear variation in the mode index where it is analysed that the mode index increases with increasing wavelength and value of lattice constant. It is clear that for smaller values of wavelength, the mode is more confined in the innermost region that is core because of the waveguide designing.

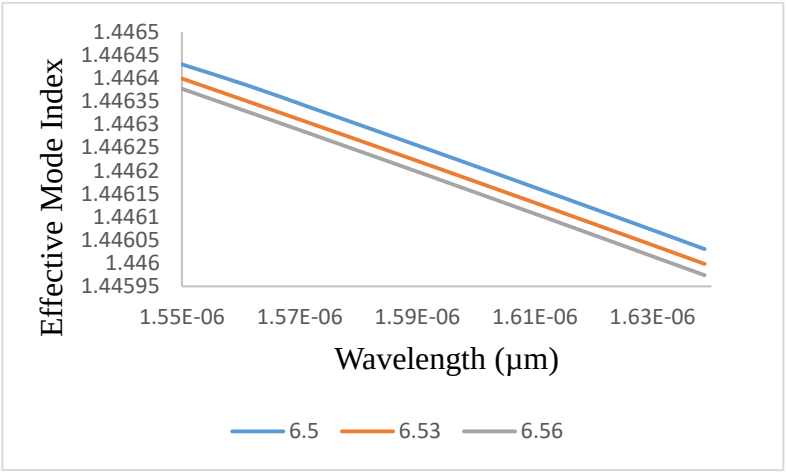

Figure 4.18 Calculated effective mode indices in the wavelength range 1.55 to 1.64 µm

Dispersion is one of the important parameter for optical communication systems as it bounds the network size. The dispersion characteristics of photonic crystal fibers can be examined by considering the refractive index of material employed and by changing the structural parameters. Dispersion is determined from effective index by:-

$$D = -(w/c\_const) * d(d(emw.n_{eff}, w), w)$$

Where n_{eff} is the effective index of the guided mode. Figure 4.19 reveals the dispersion behaviour as a function of wavelength for varying lattice constants. From the figure it can be determined that dispersion is large for greater values of lattice constants and it is following a fluctuating trend. To achieve desirable value of dispersion that is known as zero dispersion wavelength (ZDW), we have to select suitable core and cladding dimension. It is evident from the below graph that wavelength of zero dispersion escalates as the lattice constant increase.

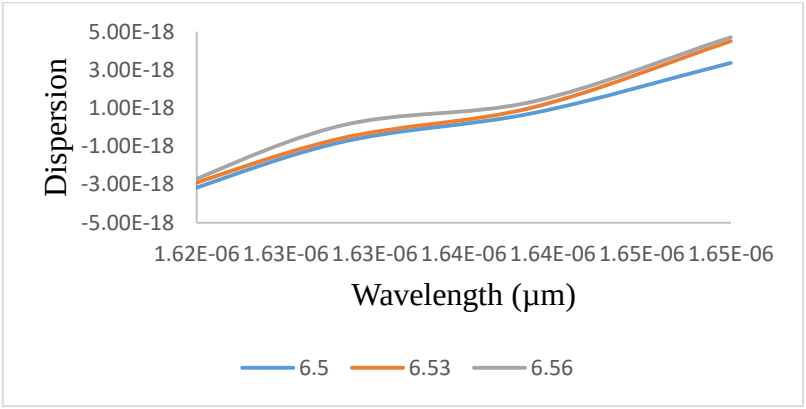

Figure 4.19 Dispersion variation with wavelength with increase in lattice constant

4.6 CONCLUSION

In this study, a PCF-based sensor consisting of seven air holes and inner layer filled with gold nanowires is designed. As the curvature of the gold nanowires is comparatively smaller than other sensors so it is easy to fill in the air holes. Finite Element Method is utilized to numerically evaluate the sensor design by employing COMSOL Multiphysics software and it is analysed that the performance of the sensor is dependent on the positioning of the design components. The simulated results reveal a low dispersion when the lattice constant is increased with a gap of 0.03μm. Our proposed PCF provided relatively higher value of electric field nearly 450 V/m with a tighter confinement of optical field than the preceding PCF structures. Thus, our presented structures of PCF has a significant advancement as compared to earlier researches as it will provide great reference for progress in real-time detection of chemicals and gases with a compact structure.

CHAPTER 5

CONCLUSION, RECOMMENDATION AND FUTURE SCOPE

5.1 CONCLUSION AND RECOMMENDATION

This chapter summarizes the results and conclusions of the defined objectives in the thesis. The research work done is concluded as follows:

The complete focus is made on designing structures based on photonic crystal fibers (PCF) by employing latest shaped structures, different hole sizes, using distinctive semiconductor materials at core and cladding regions for confining maximum light at core and obtain maximum sensitivity enhancement as achieved by variation in the RI values in the crystal fibers.

The work emphasis on two main fields- (a) elliptical resonator using metallic rod in the core; (b) a hexagonal PCF designed with gold nanorods in the innermost layer for determining the propagation characteristics.

In the first part, an elliptical resonator using metallic rods is considered. The input wavelength is taken as 1540nm. After introducing different semiconductor materials in the metallic rods and cladding region, transmission spectra was obtained for different minor axis dimensions and it was depicted that transmission efficiency cannot be enhanced beyond minor axis width of a= 4.0μm because light cannot be confined beyond these dimensions of axis. Also, with increase in minor axis along with variations in the RI, the sensitivity value is escalated. Also, about three times greater value of electric field was obtained for elliptical resonator as compared to ring resonator.

Further, enhancement in sensitivity was measured by varying the dimensions of the width of the minor axis. It was analysed that the sensitivity increases up to 10.40μm after which it is reducing. After this, addition of varying semiconductor material was done to measure the sensitivity based on the shift in the cut off wavelength as depicted due to the variation in the refractive index of the design. Sensitivity of 500nm/RIU is achieved with silicon nitride with refractive index variation from 1.56 to 1.58. Hence the sensor can be utilized for sensing various gases like nitrogen, ammonia, hydrogen etc. as refractive index of these gases is in the proximity of air.

Even, for different widths of semi minor axis and materials employed Q factor was calculated which recorded optimum value up to 626×10^3 for maximum width and silicon carbide as a material in the core region.

In the second part, we have designed a seven layered hexagonal shaped photonic crystal fiber which is employed for determining the propagation characteristics. The input wavelength is considered as 1.55μm. By adding silica in the background region and three gold nano wires in the each air hole of the inner most layer, the electric field values are recorded. The determination mechanism of the PCF is based on shift in peak resonant wavelength achieved by the change in the lattice constants. The values of electric and magnetic field distribution which has Re (N_{eff}) = 1.44594911of the guided-mode at wavelength of the incident light to be 1550nm are obtained. Further, we have visualized electric field's z-component with the help of height expression by deforming the surface in 3-D.

For determining the propagation constants, lattice constant is varied from 6.5 to 6.56μm with a difference of 0.03μm. There is linear relationship between propagation and wavelength as the value of lattice constant is varied in the defined wavelength range. It represents that the attenuation constant value increases as the lattice constant increase but decreases with increasing value of wavelength as it falls to approximately 1.80E-07 from 2.7E-07 as the wavelength increase by few micrometres.

It is analysed that the effective area falls an increasing trend with escalation in the wavelength which ranges from 1.57 to 1.64μm as depicted in Figure 4.16. The maximum value of area is $55.15\mu m^2$ that is obtained with lattice constant = 6.56μm. There is variation in the confinement loss of photonic crystal fiber as the ratio of air filling in the holes and lattice constant is altered. It is observed that as the lattice constant increases, the losses also surge. It is concluded that there is a linear variation in the mode index as the mode index increases with increasing wavelength and value of lattice constant. It is clear that for smaller values of wavelength, the mode is more confined in the innermost region that is core. On calculating the dispersion characteristics, it is depicted that there is a fluctuating trend which reveals that dispersion is large for greater values of lattice constant and smaller for reduced values of lattice constant.

5.2 FUTURE SCOPE

During the course of this research, many avenues of further continuation of this work became clear. Few of them are considered worthy and therefore, are listed below.

1. This work can be further enhanced by employing various holes shapes such as octagonal or elliptical shaped like the inner hole in elliptical in shape and circular shape of the outer holes instead of having all the holes of circular shape.

2. The photonic devices discussed in above chapters consist of silicon nitride and silicon carbide rods in the core region. Whereas, many researches of different authors are based on having colloidal solutions consisting of mixture of different components in defined ratios in aqueous form.

3. Although the sensitivity of the photonic crystal resonator discussed in chapter 3 is having good value but, it can be further improved by choosing some different material.

4. Other parameters such as figure of merit or selectivity can also be achieved which have not been discussed in the present work.

REFERENCES

[1] Khanna, Shailly. *Analysis of micro-strain sensors based on photonic crystal fibers,* Thapar University, 2015

[2] Webster John *the Measurement, Instrumentation and Sensors Handbook*. Boca Raton FL: CRC/IEEE Press, 1999.

[3] Irish Jim Instrumentation Specifications. https://ocw.mit.edu/courses/2-693-principles-of oceanographic-instrument-systems-sensors-and-measurements/ (23rd May 2017).

[4] Higuera J. M. Lopez. Optical Sensors. Spain: University of Cantabria Press, 1998.

[5] Grattan K.T.V., Sun T (2000). Fiber optic sensor technology: an overview, 82(1).40-61.

[6]PuriGaurav Optical Sensors and Their Applications: www.ee.buffalo.edu/faculty/paololiu/566/sensors.ppt (25th May 2017)

[7] Perera *et al.* (1992). Far infrared photoelectric thresholds of extrinsic semiconductor photocathodes. *Applied physics letters*, *60*(25), 3168-3170.

[8] GopelW, HesseJ, Zemel J.N, Definitions and Classifications, *Chemical and Biomedical Sensors*, 2nd ed., New York: VCH Publishers, 1991, 2.

[9] Rajan Ginu, *Optical Fiber Sensors*, New York: CRC Press- Taylor and Francis Group, 2015, 7-8.

[10] Martellucci S.,Chester A.N, and Mignani A.G, *Optical Sensors and Microsystems*, New York: Plenum Publishers, 2000,159-161.

[11] Daher, Bassam William, *Use of Sensors in Monitoring Civil Structures,* Lebanese American University, 2004.

[13] Shukla Ruchi (2014), Fiber Optic Sensors and Their Applications, International Journal of Engineering and Technical Research, 2(5), 199-201.

[14] Gupta, B D, *Fiber Optic Sensors - Principles and Applications,* New Delhi: New India Publishing Agency, 2006, 1-4.

[15] Lee Byeing Ha *et al*. (2012). Interferometric fiber optic sensors, *Sensors,* 12(3), 2467-2486.

[16] Gholamzadeh Bahareh, Nabovati Hooman (2008), Fiber Optic Sensors, International Journal of Electrical, Computer, Energetic, Electronic and Communication Engineering, 2(6), 1107-1117.

[17] Sidek Othman and Afzal Muhammad Hassan Bin (2011). A review paper on fiber-optic sensors and application of pdms materials for enhanced performance, IEEE Symposium 458-463.

[18] Maldovan Martin and Thomas Edwin L., *Periodic Materials and Interference Lithography,* Weinheim: WILEY-VCH Verlag GmbH & Co. KGaA, 2009, 141-145.

[19] Sukhoivanov Igor A. and Guryev Igor V., *Physics and Practical Modeling*, NewYork: Springer-Verlag Berlin Heidelberg, 2009, 1-5.

[20] Sharma Nidhi, Rajawat Neetu, Agrawal Kavita (2015). Photonic Crystal Fiber Characteristics Benefits Numerous Applications, International Journal of Scientific & Engineering Research, 28-33.

[21] Zaki Muhammad, Photonic Crystals, http://emt-photoniccrystal.blogspot.in/2010/05/type-of-photonic-crystal.html (25th May 2017).

[22] Xiangyong FU *et al*. (2011). Surface plasmon resonance sensor based on photonic crystal fiber filled with silver nanowires, *Optica Applicata*, 41(4), 941-951.

[23] Lu Ying *et al.* (2012). Grapefruit fiber filled with silver nanowires surface plasmon resonance sensor in aqueous environments, *Sensors*, *12*(9), 12016-12025.

[24] Peng Yang *et al. (2012).*Temperature sensor based on surface plasmon resonance within selectively coated photonic crystal fiber, *Applied optics*, *51*(26), 6361-6367.

[25] Peng Yang *et al.* (2013).Temperature sensing using the band gap-like effect in a selectively liquid-filled photonic crystal fiber, *Optics letters*, *38*(3), 263-265.

[26] Lu Y. *et al*. (2014). Temperature sensing using photonic crystal fiber filled with silver nanowires and liquid, *IEEE Photonics Journal*, *6*(3), 1-7.

[27] Luan Nannan*et al. (2014).* Surface plasmon resonance temperature sensor based on photonic crystal fibers randomly filled with silver nanowires, *Sensors*, *14*(9), 6035-16045.

[28] Du Wei and Zhao Feng (2014). Surface plasmon resonance based silicon carbide optical waveguide sensor, *Materials Letters, 115*, 92-95.

[29] Liu Qiang (2015). High-sensitivity plasmonic temperature sensor based on photonic crystal fiber coated with nanoscale gold film, *Applied Physics Express, 8*(4).

[30] Krückel Clemens J. (2015). Linear and nonlinear characterization of low-stress high-confinement silicon-rich nitride waveguides, *Optics express*, *23*(20), 25827-25837.

[31] Su Judith, Goldberg Alexander FG and Stoltz Brian M (2016). Label-free detection of single nanoparticles and biological molecules using microtoroid optical resonators, *Light: Science & Applications*, *5*(1).

[32] Liu Qiang (2016). Tunable fiber polarization filter by filling different index liquids and gold wire into photonic crystal fiber, *Journal of Light wave Technology*,*34*(10), 2484-2490.

[33] Eltes Felix (2016). Low-Loss BaTiO3–Si Waveguides for Nonlinear Integrated Photonics, *ACS Photonics*, *3*(9), 1698-1703.

[34] Witmer Jeremy D, Hill Jeff T., and Safavi-Naeini Amir H. (2016). Design of nanobeam photonic crystal resonators for a silicon-on-lithium-niobate platform, *Optics express, 24*(6), 5876-5885.

[35] Chao Liu *et al. (2017).* Numerical analysis of a photonic crystal fiber based on a surface plasmon resonance sensor with an annular analyte channel, Optics *Communications, 382*, pp.162-166.

[36] Huq Md. Faizul*et al.* (2016). Design and optimization of photonic crystal fiber for liquid sensing applications, *Photonic Sensors, 6*(3), 279-288.

[37] Yang X. C *et al.* (2016). Temperature Sensor Based on Photonic Crystal Fiber Filled With Liquid and Silver Nanowires, *IEEE Photonics Journal, 8*(3), 1-9.

[38] Narayan Jitendra, Dash, and Jha Rajan (2014). SPR biosensor based on polymer PCF coated with conducting metal oxide, *IEEE Photonics Technology Letters, 26*(6), 595-598.

[39] Huang Min *et al.* (2009). Sub-wavelength nanofluidics in photonic crystal sensors", *Optics express, 17*(26), 24224-24233.

[40] X.C. Yang *et al. (2015).* A photonic crystal fiber glucose sensor filled with silver nanowires, *Optics Communications, 359*, 279-284.

[41] Saboo, Shweta, and Gupta Chandra Prakash (2013). Design of Photonic Crystal Fiber For Minimum Confinement Loss By Varying The Size Of Holes, *International Journal of Electronics and Communication Engineering (IJECE), 2* (2).

[42] Zhu Hongying *et al.* (2007). Analysis of bio molecule detection with opto- fluidic ring resonator sensors, *Optics Express, 15*(15), 9139-9146.

[43] Hao Feng *et al.* (2009). Tunability of subradiant dipolar and Fano-type plasmon resonances in metallic ring/disk cavities: implications for nanoscale optical sensing, ACS *nano, 3*(3), 643-652.

[44] Sun Yuze and Fan Xudong (2011). Optical ring resonators for biochemical and chemical sensing. *Analytical and bio analytical chemistry, 399*(1), 205-211.

[45] Feng Lishuang *et al*. (2014). Transmissive resonator optic gyro based on silica waveguide ring resonator, *Optics express,* 22(22), 27565-27575.

[46] Dolatabady Alireza, Granpayeh Nosrat, Nezhad Vahid Foroughi (2013). A nanoscale refractive index sensor in two dimensional plasmonic waveguide with nanodisk resonator, *Optics Communications, 300,* 265-268.

[47] Fan X Z *et al. (*2015).Porous silicon ring resonator for compact, high sensitivity bio sensing applications, *Optics express,* 23.6, 7111-7119.

[48] Rodriguez Gilberto A, Hu Shuren, and. Weiss Sharon M (2010).Continuous wave photon pair generation in silicon-on-insulator waveguides and ring resonators: erratum. *Optics Express,* 18(13), 14107-14107.

[50] Zheng Shaonan *et al.* (2016). High-resolution on-chip spectrometer with a tunable micro-ring resonator filter, Lasers and Electro-Optics (CLEO), 16543248: CA, USA: 19 December, 2016, 1-2.

[51] Rotenber Nir *et al*. (2017). Small slot waveguide rings for on-chip quantum optical circuits, *Optics Express*, 25(5), 5397-5414.

[52] Ademgil. H., &Haxha, S. (2008). Highly birefringent photonic crystal fibers with ultralow chromatic dispersion and low confinement losses. *Journal of lightwave technology*, *26*(4), 441-448.

[53] Hameed Mohamed Farhat O. *et al.* (2009). Modal properties of an index guiding nematic liquid crystal based photonic crystal fiber. *Journal of Lightwave Technology*, *27*(21), 4754-4762.

[54] Faruk Md. Omar *et al.* (2010). Effect of lattice constant and air hole diameter on the mode profile in triangular and square lattice photonic crystal fiber at THz regime. In *Proceedings of the World Congress on Engineering and Computer Science*, 2, 1109-1114.

[55] Mc Elhenny *et al.* (2011). Dependence of frequency shift of depolarized guided acoustic wave Brillouin scattering in photonic crystal fibers. *Journal of Lightwave Technology*, *29*(2), 200-208.

[56] Revathi S. *et al.* (2012). Analysis of propagation characteristics in photonic crystal fiber structure for large negative dispersion, Journal of Theoretical and Applied Information Technology, 36(1), 129-133.

[57] Dudley *et al.* (2006). Supercontinuum generation in photonic crystal fiber. *Reviews of modern physics*, *78*(4), 1135.

[58] Hossain Md. Sajjad *et al.* (2014). Dispersion and nonlinear characteristics of a photonic crystal fiber (PCF) with defected core and various doping concentration. In *Electrical and Computer Engineering (ICECE), 2014 International Conference*,Dhaka, Bangladesh, 20-22 December, 2014, 500-503.

[59] Nair AA *et al*. (2014). Comparative study of octagonal ring photonic crystal fiber with GeO_2 doped structure, in *Information Communication and Embedded Systems (ICICES), 2014 International Conference:* 27 February, 2014, 1-6.

[60] Saghaei Hamed *et al.* (2015). Mid infrared super continuum generation via As_2Se_3chalcogenide photonic crystal fibers. *Applied optics*, *54*(8), 2072-2079.

[61] Hong Kee Suk *et al.* (2016). Analysis on Transition between Index- and Bandgap-guided Modes in Photonic Crystal Fiber, *Journal of the Optical Society of Korea*, *20*(6), 733-738.

[62] Siwicki Bartłomiej *et al.* (2017). Nanostructured graded-index core chalcogenide fiber with all-normal dispersion–design and nonlinear simulations, *Optics Express*, 11, 12984-12998.

[63] MA J. *et al.* (2017). High-performance temperature sensing using a selectively filled solid-core photonic crystal fiber with a central air-bore. *Optics Express*, *25*(8), 9406-9415.

[64] FlanneryJeremy *et al.* (2017). Implementing Bragg mirrors in a hollow-core photonic-crystal fiber. *Optical Materials Express, 7*(4), 1198-1210.

[65] CassataroMarco *et al.* (2017). Generation of broadband mid-IR and UV light in gas-filled single-ring hollow-core PCF, *Optics Express*, *25*(7), 7637-7644.

[66] Chupao Lin *et al.* (2017). Liquid modified photonic crystal fiber for simultaneous temperature and strain measurement. *Photonics Research, 5*(2), 129-133.

[67] Hasan Rakibul *et al. (2015).* Extraction of Modeling Parameters for Low-loss Alternative Plasmonic Material, *Elsevier*,195,2061-2066.

[68] Arefin Riazul *et al.* (2016). Design of a Tunable Ring Resonator with Enhanced Quality Factor, In Electrical and Computer Engineering (ICECE), 9th Conference: Dhaka,Bangladesh: 20 December, 2016, 369-372.

[69] Dolatabady Alireza *et al.* (2013). A nano scale refractive index sensor in two dimensional plasmonic waveguide with nanodisk resoantor, Elsevier,365-368.

[70] Zhu H *et.al. (2007).* Analysis of bio molecule detection with opto-fluidic ring resonator sensors, *Optics Express*, 15(15), 9139-9146.

[71] Dolatabady *et al.* (2013).A nanoscale refractive index sensor in two dimensional plasmonic waveguide with nanodisk resonator, Optics Communications, 300, 265-268.

[72] Sun, Yuze, and Fan Xudong (2011).Optical ring resonators for biochemical and chemical sensing, Analytical and bioanalytical chemistry, 399(1), 205-211.

[73] Russell, Philip St J (2006). Photonic crystal fibers, *J. Lightw. Technol.*, 24(12), 4729–4749.

[74] Dash Jitendra Narayan and Jha Rajan (2014). Surface plasmon resonance biosensor based on polymer photonic crystal fibers coated with conducting metal oxide, *IEEE Photon. Technol. Lett*., 26(6), 595–598.

[75] Kuhlmey *et al.* (2009). Fluid-filled solid-core photonic bandgap fibers, *Journal of Lightwave Technology*, 27(11), 1617–1630.

[76] Yongqin Yu *et al*. (2010). Some features of the photonic crystal fiber temperature sensor with liquid ethanol filling, *Optics Express*, 18(15), 15383–15388.

[77] Qiu Sun-jie *et al*. (2012). Temperature sensor based on an isopropanol-sealed photonic crystal fiber in-line interferometer with enhanced refractive index sensitivity, *Optics Letters*, 37(5), 863–865.

[78] Liu Qiang *et al.* (2015). Photonic crystal fiber temperature sensor based on coupling between liquid-core mode and defect mode, *IEEE Photonics Journal*, vol. 7(2), 1-9.

[79] Chen Hailiang *et al. (2014).* High sensitivity of temperature sensor based on ultra-compact photonics crystal fibers, *IEEE Photonics Journal*, 6(6), 1-6.

[80] Larsen Thomas Tanggaard *et al*. (2003). Optical devices based on liquid crystal photonic bandgap fibres, *Optics Express*, 11(20), 2589–2596.

[81] Villatoro Joel, Finazzi Vittoria, and Pruneri Valerio, (2011), Functional photonic crystal fiber sensing devices, SPIE: 12784361: Shanghai, China: 13-16 November, 2011, 1–6.

[82] Villataro Joel *et al.* (2007).Temperature-insensitive photonic crystal fiber interferometer for absolute strain sensing, *Applied Physics Letters*, 91(9).

[83] Liu Bing Hong *et al*. (2013). Hollow fiber surface plasmon resonance sensor for the detection of liquid with high refractive index, *Optics Express*, 21(26), 32349–32357.

[84] Fan Zhenkai *et al*. (2015). High sensitivity of refractive index sensor based on analytic-filled photonic crystal fiber with surface plasmon resonance," IEEE Photon. J., vol. 7(3), 1-9.

[85] Zu Peng *et al*. (2011). A temperature-insensitive twist sensor by using low-birefringence photonic-crystal-fiber-based Sagnac interferometer, *IEEE Photonic Technology Letters*, 23(13), 920–922.

[86] Chen Hailing *et al*. (2015). Magnetic field sensor based on magnetic fluid selectively infilling photonic crystal fibers, *IEEE Photonic Technology Letters*, 27, 717–720.

[87] Zhang Haiwei *et al*. (2014). Intracavity absorption multiplexed sensor network based on dense wavelength division multiplexing filter, *Optics Express*, 22(20), 24545–24550.

[88] Gurpreet Kaur, R. S. Kaler, Naveen Kwatra (2016). On the optimization of fiber Bragg grating optical sensor using genetic algorithm to monitor the strain of civil structure with high sensitivity", Optical engineering, Optical Engineering, 55(8), 087103-1 to 087103-6.

[89] Peng Yang *et al*. (2012). Temperature sensor based on surface plasmon resonance within selectively coated photonic crystal fiber, *Applied Optics*, 51(26), 6361–6367.

[90] Liu Qiang *et al.* (2015). High-sensitivity plasmonic temperature sensor based on photonic crystal fiber coated with nanoscale gold film, *Applied Physics Express*, vol. 8(4).

[91] Csaki Andrea *et al*. (2010). Nanoparticle layer deposition for plasmonic tuning of micro structured optical fibers, Small, 6(22), 2584–2589.

[92] Peng Yang *et al*. (2013). Temperature sensing using the band gap-like effect in a selectively liquid-filled photonic crystal fiber, *Optic Letters*, 38(3), 263–265.

[93] Lu Y. *et al.* (2014). Temperature sensing using photonic crystal fiber filled with silver nanowires and liquid, *IEEE Photonic Journal*, 6(3), 1-7.

[94] Gurpreet Kaur and R.S. Kaler (2017). Design and performance evaluation of hybrid optical sensor, Optik, (140), 508–514.

[95] Gurpreet Kaur, R. S. Kaler, Naveen Kwatra. (2017). Investigations on highly sensitive fiber Bragg gratings with different grating shapes for far field applications, 131,483–489.